



Proposed standardized definitions for vertical resolution and uncertainty in the NDACC lidar ozone and temperature algorithms. Part 1: Vertical resolution

5 Thierry Leblanc¹, Robert J. Sica², J. Anne E. van Gijsel³, Sophie Godin-Beekmann⁴,
Alexander Haeferle⁵, Thomas Trickl⁶, Guillaume Payen⁷, and Frank Gabarrot⁷

¹Jet Propulsion Laboratory, California Institute of Technology, Wrightwood, CA 92397, USA

²Department of Physics and Astronomy, The University of Western Ontario, London, Canada

³Royal Netherlands Meteorological Institute (KNMI), Netherlands

⁴LATMOS-IPSL, CNRS-INSU, Paris, France

10 ⁵Meteoswiss, Payerne, Switzerland

⁶Karlsruher Institut für Technologie, IMK-IFU, Garmisch-Partenkirchen, Germany

⁷Observatoire des Sciences de l'Univers de La Réunion, CNRS and Université de la Réunion (UMS3365), Saint Denis de la Réunion, France

Correspondence to: Thierry Leblanc (thierry.leblanc@jpl.nasa.gov)

15 Abstract. A standardized approach for the definition and reporting of vertical resolution of the ozone and temperature lidar profiles contributing to the Network for the Detection for Atmospheric Composition Change (NDACC) database is proposed. Two standardized definitions describing homogeneously and unequivocally the impact of vertical filtering are recommended.

The first proposed definition is based on the width of the response to a Finite Impulse-type perturbation. The response is computed by convolving the filter coefficients with an impulse function, namely, a Kronecker Delta function for smoothing filters, and a Heaviside Step function for derivative filters. Once the response has been computed, the proposed standardized definition of vertical resolution is given by $\Delta z = \delta z * H_{FWHM}$, where δz is the lidar's sampling resolution and H_{FWHM} is the full-width at half-maximum (FWHM) of the response, measured in sampling intervals.

25 The second proposed definition relates to digital filtering theory. After applying a Laplace Transform to a set of filter coefficients, the filter's gain characterizing the effect of the filter on the signal in the frequency-domain is computed, from which the cut-off frequency f_c , defined as the frequency at which the gain equals 0.5, is computed. Vertical resolution is then defined by $\Delta z = \delta z / (2f_c)$. Unlike common practice in the field of spectral analysis, a factor $2f_c$ instead of f_c is constrained here to yield vertical resolution values nearly equal to the values obtained with the impulse response definition using the same filter coefficients. When using either of the proposed definitions, unsmoothed signals yield the best possible vertical resolution $\Delta z = \delta z$ (one sampling bin).

30 Numerical tools were developed to support the implementation of these definitions across all NDACC lidar groups. The tools consist of ready-to-use "plug-in" routines written in several programming languages that can be inserted into any lidar data processing software and called each time a filtering operation occurs in the data processing chain.



1 Introduction

As part of the Network for the Detection of Stratospheric Composition Change (NDACC), over 20 ground-based lidar instruments are dedicated to the long-term monitoring of atmospheric composition and to the validation of space-borne measurements of Earth's atmosphere from environmental satellites (e.g., EOS-Aura, ENVISAT, NPP, the Sentinels). In networks such as NDACC, the instruments use a wide spectrum of methodologies and technologies to measure key atmospheric parameters such as ozone, temperature, water vapor, etc. One ensuing caveat is the difficulty to archive measurement and analysis information consistently within all research groups or instruments. Yet the need for consistent definitions has strengthened as datasets of various origin (e.g., satellite and ground-based) need increased quality control and thorough validation before they can be used for long-term trend studies or be ingested together in global assimilation systems. For example, recommendations were recently made for the use of specific effective vertical resolution schemes within the European Aerosol Research Lidar Network (EARLINET; Iarlori et al., 2015), and efforts were made to produce aerosol lidar data with a certain level of standardization (D'Amico et al., 2015). Within the NDACC Lidar Working Group, a few studies have shown the impact on ozone of using different definitions of vertical resolution (e.g., Beyerle and McDermid, 1999; Godin et al., 1999), or have estimated the impact of various corrections on temperature (e.g., Leblanc et al., 1998), but little work was done to facilitate a standardization of the definitions and approaches relating to vertical resolution and uncertainty budget in NDACC lidar retrievals.

In order to address such need for consistency, several NDACC lidar collaborators have joined forces through the formation in 2011 of an *International Space Science Institute* (ISSI) International Team of Experts (<http://www.issibern.ch/aboutissi/mission.html>). The objective of this working group (henceforth "ISSI Team") was to provide scientifically meaningful recommendations for the use of standardized definitions of vertical resolution and standardized definitions and approaches for the treatment of uncertainty in the NDACC ozone and temperature lidar retrievals. Ultimately, the recommendations, as compiled in the ISSI Team Report (Leblanc et al., 2016a), were designed so that they can be implemented consistently by all NDACC ozone and temperature lidar investigators.

The present article is the first of three companion papers that provide a comprehensive description of the recommendations made by the ISSI Team to the NDACC lidar community for the standardization of vertical resolution and uncertainty. The present article (Part 1) is exclusively dedicated to the description of the proposed standardized vertical resolution. A second paper (Part 2) (Leblanc et al., 2016b) reviews the proposed standardized definitions and approaches for the ozone differential absorption lidars uncertainty budget. The last paper (Part 3) (Leblanc et al., 2016c) reviews the proposed standardized definitions and approaches for the NDACC temperature lidars uncertainty budget. Details that appear beyond the scope of the present three companion papers may be found in the ISSI Team Report (Leblanc et al., 2016a).

Though the ISSI Team focus has been on the retrieval of ozone by the differential absorption technique (Mégie et al., 1977), and temperature by the density integration technique (Hauchecorne and Chanin, 1980; Arshinov et al., 1983), most recommendations made in the present and two companion papers can be followed for the retrieval of other NDACC lidar species such as water vapor (Raman and differential absorption techniques), temperature



(rotational Raman technique), and aerosol backscatter ratio. One exception is when using an Optimal Estimation Method (OEM) for the retrieval of temperature as recently proposed by Sica and Haeferle (2015), for which vertical resolution is implicitly determined from the full-width at half-maximum of the OEM's averaging kernels.

Vertical resolution, as provided in the lidar data files, is an indicator of the amount of vertical filtering applied to the lidar signals or to the measured species profiles. This filtering is applied in order to reduce high frequency noise typically produced at the signal detection level. A higher vertical resolution means that the instruments is able to detect features of small vertical extent, while a lower vertical resolution implies a reduced ability to detect features of small vertical scale. Typically, vertical resolution is provided in a unit of vertical length (e.g., meter). Because the lidar signal-to-noise ratio strongly varies with altitude, the amount of filtering typically applied also varies with altitude, with more filtering applied at higher altitude ranges.

Here the word *filtering* is preferred to the word *smoothing* because it is more general and applies to both smoothing and differentiation processes, the former process being relevant to both temperature and ozone lidar retrievals, and the latter process being relevant to the ozone differential absorption technique. To optimize the useful range of lidar measurements, most lidar signals or profiles are digitally filtered at some point in the retrieval process. Over the years, NDACC lidar investigators have been providing temperature and ozone profiles using a wide range of vertical resolution schemes and values, where the definition of vertical resolution appears to differ significantly. The objective of the present work is not to recommend a specific vertical resolution scheme, but instead to ensure that the definition used by the data provider to describe his scheme is reported and interpreted consistently across the entire network. The approaches and recommendations in this article were designed so that they can be implemented consistently by all NDACC lidar investigators and beyond (e.g., the Tropospheric Ozone Lidar Network, TOLNet, or the GCOS Reference Upper Air Network, GRUAN). We therefore recommend two well-known definitions, one definition based on the full-width at half-maximum of a finite impulse response, and the other definition based on the cut-off frequency of digital filters. These definitions allow a clear mapping of the amount of filtering applied to the lidar signal or species profile with the values of vertical resolution actually reported in the data files.

Section 2 summarizes the basics of digital signal filtering, and provides a few examples of how vertical resolution can be expressed in terms of impulse response and digital filter cut-off frequency. **Section 3** reviews a number of vertical resolution definitions used by the NDACC ozone and temperature lidar community. The results from **sections 2 and 3** are used in **section 4** to recommend and detail two practical, well-known definitions of vertical resolution that can be easily linked to the underlying filtering processes. The numerical values of vertical resolution computed using these two definitions are compared for several types of digital filters. For the sake of completeness, a supplement to the present manuscript provides additional characteristics of several commonly-used smoothing and derivative filters.

Numerical tools were developed by the ISSI Team to facilitate the implementation of the proposed standardized definitions. The tools consist of subroutines written in four scientific languages (IDL, MATLAB, FORTRAN and Puython) which can be inserted in the lidar investigators' data processing softwares in order to compute the proper, standardized numerical values of vertical resolution. The plug-in routines are available upon request to the first author (thierry.leblanc@jpl.nasa.gov).



2 Brief review of signal filtering theory

In this section we do not pretend to reinvent the wheel. We simply review the mathematical background that allows us to link vertical resolution to the lidar signal (or profile) filtering process. Signal filtering for lidar data processing consists of either smoothing, differentiating or smoothing and differentiating at the same time. To describe the filtering process a signal S is defined in its general sense, i.e., it can be either a raw lidar signal from a single detection channel, or the ratio of the corrected signals from two detection channels, or an unsmoothed ozone profile, temperature profile, calibrated or uncalibrated water vapor profile, etc. The only common requirement is that the signal is formed of a finite number of equally-spaced samples in the vertical dimension $S(k)$ with $k=[1, nk]$. The constant interval between two samples, $\delta z = z(k+1)-z(k)$ for all k , is the *sampling width*, or *sampling resolution*, and corresponds to the smallest vertical interval that can be resolved by the lidar instrument.

In its most physical sense, the signal filtering process at an altitude $z(k)$ consists of convolving a set of $2N+1$ coefficients c_n with the signal S over the interval $\Delta z = 2N\delta z$ of boundaries $z(k-N)$ and $z(k+N)$ (e.g., Hamming, 1989):

$$S_f(k) = \sum_{n=-N}^N c_n S(k+n) \quad (1)$$

where S_f is the signal after filtering. The transformation associated with this process is known as a non-recursive digital filter the simplest kind of digital filters, with the coefficients c_n being the coefficients of the filter. A simple example is the arithmetic average for which all coefficients take the same value $c_n = 1/(2N+1)$. Several other filter names exist for this particular example, for example boxcar smoothing filter, boxcar function, or smoothing by $[2N+1]s$ (Hamming, 1989).

The number of filter coefficients and the values of these coefficients determine the actual effect of the filter on the signal. Three critical aspects of the effect of the filter on the signal are 1) the amount of noise reduction due to filtering, 2) the nature and degree of symmetry/asymmetry of the coefficients around the central value which determines whether the filter's function is to smooth, sum, differentiate, or interpolate, and 3) whether the magnitude of specific noise frequencies are being amplified or reduced after filtering. In the particular case of an unfiltered signal comprised of independent samples and assuming that the variance of the noise for the unfiltered signal is constant through the filtering interval considered ($\sigma_s^2(k') = \sigma^2$ for all k' in the interval $[k-N, k+N]$), we obtain a simple relation that estimates the variance of the output signal:

$$\sigma_{sf}^2(k) = \sigma_s^2 \sum_{n=-N}^N c_n^2 \quad (2)$$

This relation reveals the importance of the sum of the squared-coefficients to determine the amount of noise reduction. However, it does not provide any information on the ability of the filter to distinguish what is noise and what is actual signal. To illustrate this problem, **Fig. 1** shows an example of a noisy signal before and after filtering, considering two different filters. We start from a modeled signal represented by the green dash-dot curve. To this ideal signal, we add random noise which amplitude is distributed following the Poisson statistics (signal detection noise). The noisy "unfiltered" signal is represented in this figure by a dark-grey dotted curve. The signal is then filtered using two different filters, i.e., two different sets of coefficients. The blue curve shows the filtered signal



using least squares linear fitting (identical to boxcar average, labeled LS-1), while the red curve shows the filtered signal this time using least squares fitting with a polynomial of degree 2 (LS-2). The number of terms used by both filters is the same ($2N+1=11$). The values of the coefficients, and not the number of coefficients, are responsible for the observed difference.

5 In the real world, we typically do not know the exact nature or behavior of the measured signal. Consider the example in **Fig. 1**, if the definition used to report vertical resolution in the data files was based on the number of points used by the filter, we would not be able to attribute the differences observed between the blue and red curves to a difference in the filtering procedure. We therefore need to find some analytical way to characterize a specific filter if we want to understand its exact effect on the signal, and properly interpret features observed on the smoothed signal. We will see thereafter that it is indeed possible to determine the resolution of the filter by either
 10 quantifying the response of a controlled impulse in the physical domain, or by using a frequency approach and studying the frequency-response of the filter.

2.1 Classical approach: Unit impulse response and unit step response

The impact of a specific filter on the signal can be characterized by computing the unit impulse response in the
 15 physical domain (usually called the time domain in time series analysis). This can be done by using a well-known, controlled input signal, e.g., an impulse, and by studying its response after being convolved by the filter coefficients. Considering a finite impulse response is equivalent to considering the output signal I_{OUT} formed by the convolution of an impulse I_{INP} with a finite number of coefficients c_n :

$$I_{OUT}(k) = \sum_{n=-N}^N c_n I_{INP}(k+n) \quad (3)$$

20 For smoothing, non-derivative filters, this impulse is the discrete Kronecker delta function δ_{k_0} (also called unit impulse function), which takes a value of 1 at coordinate $k=k_0$ and 0 elsewhere:

$$\begin{aligned} \delta_{k_0}(k) &= 1 && \text{for } k = k_0 \\ \delta_{k_0}(k) &= 0 && \text{for all } k \neq k_0 \end{aligned} \quad (4)$$

Using our smoothing interval of $2N+1$ points centered at altitude $z(k)$, the input impulse for which the response is
 25 needed will have a value of 1 at the central point, and 0 at all other points:

$$\begin{aligned} I_{INP}(k+n) &= 1 && \text{for } n = 0 \\ I_{INP}(k+n) &= 0 && \text{for } 0 < |n| \leq N \end{aligned} \quad (5)$$

For derivative filters, it is more adequate to calculate the response of a discrete Heaviside step function H_S (also called unit step function), which takes a value of 0 for all strictly negative values of k , and a value of 1 elsewhere:

$$\begin{aligned} H_S(k) &= 0 && k < 0 \\ H_S(k) &= 1 && k \geq 0 \end{aligned} \quad (6)$$



Again using an interval of $2N+1$ points centered at $z(k)$, the input step for which the response is needed will have a value of 0 for all samples below the central point $z(k)$, and a value of 1 for the central point and all samples above it:

$$\begin{aligned} I_{INP}(k+n) &= 0 & -N \leq n < 0 \\ I_{INP}(k+n) &= 1 & 0 \leq n \leq N \end{aligned} \quad (7)$$

5 Though we considered an impulse (delta function) for smoothing filters and a step function (Heaviside step) for the derivative filters, for brevity we will call both types of response an “*impulse response*” in the rest of this article. For each altitude location considered, the impulse response consists of a vector which length is at least as large as twice the number of filter coefficients used to smooth the signal at this location. The magnitude of the impulse response typically maximizes at the central point $z(k)$ of the filtering interval, and then decreases apart from this central value
 10 to a value of 0 for points outside the smoothing interval. Unlike the number of coefficients used by the filter, the width of the response (measured in number of bins) provides a quantitative measure of the actual smoothing impact of the filter on the signal at this location. The impulse response of a boxcar average is shown in **Fig. 2** for several filter widths. Additional examples of impulse response for several smoothing and derivative filters are provided throughout this article and in the Supplement. Later in this paper, we will link vertical resolution as it is often
 15 reported in lidar data files to the impulse response width, and more precisely to its full-width-at-half-maximum (FWHM) (see **sections 3 and 4**).

2.2 The frequency approach: Transfer function and gain

As in many signal processing applications, the frequency approach applied to lidar signal filtering or lidar-retrieved profile filtering is a very convenient mathematical framework. It is a more abstract, but very powerful tool allowing
 20 to understand many hidden features of the smoothing and differentiation processes. A succinct, yet clear discussion of the required mathematical background is provided by Hamming (1989). Here, we will provide a brief review of this background relevant to our applications.

1) *Aliasing*: Any signal consisting of a finite number of equally-spaced samples in the physical domain is an aliased representation of a sine and cosine function of frequency ω . Using the usual trigonometry formulae and the Euler identity, we can therefore express a single-frequency signal with unity amplitude in complex form:
 25

$$S(k) = e^{i\omega k} \quad (8)$$

In the case of lidar, the signal (or the ozone or temperature profile) is a function of altitude range. The discretized independent variable is the vertical sampling bin k . The angular frequency ω (unit: radian.bin⁻¹) is then connected to the frequency f (unit: bin⁻¹) and vertical wavelength L (unit: bin) by the relations:

$$30 \quad \omega = 2\pi f = \frac{2\pi}{L} \quad (9)$$

2) *Eigen-functions and eigenvalues of a linear system*: Any vector \mathbf{x} of length M can be formed by linear combination of M linearly independent (orthogonal) eigenvectors \mathbf{x}_i :

$$\mathbf{x} = \sum_{i=1}^M a_i \mathbf{x}_i \quad (10)$$



Furthermore, any non-zero and non-unity matrix \mathbf{A} of dimension M by M multiplied by this vector can be expressed as the sum of the products of its elements by the corresponding eigenvalues λ_i :

$$\mathbf{Ax} = \sum_{i=1}^M a_i \mathbf{Ax}_i = \sum_{i=1}^M a_i \lambda_i \mathbf{x}_i \quad (11)$$

3) *Invariance under translation*: The property of invariance under translation for the sine and cosine functions implies a direct relation between the signal expressed in its complex form and the eigenvalue $\lambda(\omega)$ for a given translation:

$$S(k+n) = e^{i\omega(k+n)} = e^{i\omega n} e^{i\omega k} = \lambda(\omega) S(k) \quad (12)$$

Using the above mathematical background, the filtered signal S_f presented in its classical form as a linear combination of the input signal S (**Eq. (1)**) can be re-written in its frequency-approach form:

$$10 \quad S_f(k) = e^{i\omega k} \sum_{n=-N}^N c_n e^{i\omega n} = \lambda(\omega) e^{i\omega k} = \lambda(\omega) S(k) \quad (13)$$

The eigenvalue $\lambda(\omega)$ is independent of k , and is called the *transfer function*, which can be computed in the frequency domain over a full cycle $[-\pi, \pi]$, or over half a cycle $[0, \pi]$ without losing information (symmetry of translation):

$$\lambda(\omega) = \sum_{n=-N}^N c_n e^{i\omega n} \quad 0 \leq \omega \leq \pi \text{ radian} \cdot \text{bin}^{-1} \quad (14)$$

We can express the transfer function more conveniently as a function of the frequency f :

$$15 \quad H(f) = \sum_{n=-N}^N c_n e^{2i\pi f n} \quad 0 \leq f \leq 0.5 \text{ bin}^{-1} \quad (15)$$

The maximum value $f = 0.5 \text{ bin}^{-1}$ is the Nyquist frequency, which corresponds to $L=2$ bins, and which expresses the fact that the lidar instrument is unable to exactly reproduce any feature of vertical wavelength smaller than twice the sampling resolution ($2\delta z$). The transformation described in **Eq.**

(15) can easily be recognized as a well-known discrete Laplace Transform, applied to the filter coefficients.

For a typical smoothing filter, the coefficients have even symmetry, i.e., $c_n = c_{-n}$ for all values of n . The complex transfer function can then be reduced to its real part. The gain of the filter G , which is the ratio of the actual transfer function $H(f)$ to the ideal transfer function $I(f)$ can then be written:

$$G(f) = \frac{H(f)}{I(f)} = \frac{H(f)}{1} = c_0 + 2 \sum_{n=1}^N c_n \cos(2\pi n f) \quad 0 \leq f \leq 0.5 \text{ bin}^{-1} \quad (16)$$

25 For a derivative filter, the $2N+1$ coefficients have odd symmetry, i.e., $c_n = -c_{-n}$ for all values of n and $c_0 = 0$. The complex transfer function is then reduced to its imaginary component:

$$H(f) = 2i \sum_{n=1}^N c_n \sin(2\pi n f) \quad (17)$$

With the complex notation of **Eq. (8)**, the ideal vertical derivative of the signal can be written:



$$S_f(k) = i\omega e^{i\omega k} = 2i\pi f e^{i\omega k} \quad (18)$$

The gain of the filter, i.e., the ratio of the actual transfer function to the ideal transfer function, then takes the form:

$$G(f) = \frac{H(f)}{2i\pi f} = \frac{1}{\pi f} \sum_{n=1}^N c_n \sin(2\pi n f) \quad 0 \leq f \leq 0.5 \text{ bin}^{-1} \quad (19)$$

The gain provides a quantitative measure of the actual smoothing impact of the filter on the signal at a particular location $z(k)$ and for a given spectral component f .

Examples of gain for several smoothing and derivative filters are shown in **Fig. 2 (right)**, and throughout the rest of this article as well as in the Supplement. Just like for the impulse response, later in this paper we will link vertical resolution as it is often reported in lidar data files to the cut-off frequency of digital filters, which is computed from the gain (see **sections 3 and 4**).

2.3 Example 1: Least squares fitting, boxcar average, and smoothing by ns

Least-squares fitting is a well-established numerical technique used for many applications such as signal smoothing, differentiation, interpolation, etc.. The relation between the number and values of the filter coefficients and the type of polynomial used to fit the signal can be found in many text books and publications (e.g., Birge and Weinberg, 1947; Savitsky and Golay, 1964; Steinier et al., 1972). In this paragraph we show that *least-squares fitting* with a straight line, *boxcar averaging* and *smoothing by ns* , are all the same filter. We start with the simple case of fitting five points with a straight line. We therefore look for the minimization of the following function:

$$F(a_0, a_1) = \sum_{n=-2}^2 [S(k+n) - (a_0 + a_1 n)]^2 \quad (20)$$

This minimization is done by differentiating F with respect to each coefficient a_0 and a_1 and finding the root of each corresponding equation:

$$\begin{cases} 5a_0 + 0a_1 = \sum_{n=-2}^2 S(k+n) \\ 0a_0 + 10a_1 = \sum_{n=-2}^2 nS(k+n) \end{cases} \quad (21)$$

The value of the signal after filtering S_f is the mid-point value of the fitting function $a_0 + a_1 n$ which corresponds to the value of a_0 ($n=0$):

$$S_f(k) = a_0 = \frac{1}{5} \sum_{n=-2}^2 S(k+n) \quad (22)$$

Identifying this equation to the generic **Eq. (1)**, we deduce the five coefficients of the filter:

$$c_n = \frac{1}{5} \quad -2 \leq n \leq 2 \quad (23)$$

We recognize the smoothing-by-5s filter or 5-point boxcar average, or 5-pts running average. The impulse response of this filter takes a value of 1 for all $|n|$ comprised between 0 and N , and a value of 0 elsewhere (see **Fig. 2** left plot).



Not surprisingly, all impulse response curves maximize at the central point ($n=0$), and their full-width at half-maximum (FWHM) increases with the number of filter coefficients used.

Now switching to the frequency domain and using **Eq. (14)**, the transfer function $\lambda(\omega)$ can be written in complex form:

$$5 \quad \lambda(\omega) = \frac{1}{5} [e^{-2i\omega} + e^{-i\omega} + 1 + e^{i\omega} + e^{2i\omega}] \quad (24)$$

The gain of the filter can be expressed as a function of frequency f :

$$G(f) = H(f) = \frac{1}{5} + 2 \sum_{n=1}^2 \frac{1}{5} \cos(2\pi n f) \quad (25)$$

which simplifies to:

$$G(f) = H(f) = \frac{1}{5} \left[\frac{\sin(5\pi f)}{\sin(\pi f)} \right] \quad (26)$$

10 We can generalize the above equation by fitting $2N+1$ points with a straight line, and we find:

$$c_n = \frac{1}{2N+1} \quad -N \leq n \leq N \quad (27)$$

$$\lambda(\omega) = \frac{1}{2N+1} [e^{-Ni\omega} + e^{-(N-1)i\omega} + \dots + e^{-i\omega} + 1 + e^{i\omega} + \dots + e^{(N-1)i\omega} + e^{Ni\omega}] \quad (28)$$

Or in function of frequency:

$$G(f) = H(f) = \frac{1}{2N+1} + 2 \sum_{n=1}^N \frac{\cos(2\pi n f)}{2N+1} \quad (29)$$

15 which simplifies to

$$G(f) = H(f) = \frac{1}{2N+1} \left[\frac{\sin((2N+1)\pi f)}{\sin(\pi f)} \right] \quad (30)$$

The gain functions for smoothing by 3s through 25s filters are plotted on the right-hand side of **Fig. 2**. The gain provides a more complete description of the smoothing ability of the filters because it provides a measure of noise attenuation as a function of frequency. All curves show a gain close to 1 for frequency values near 0 (low-pass filters), but they also show large wiggles at larger frequencies when we approach the Nyquist frequency. The frequency f_0 of the first zero-crossing (zero-gain) is determined by the number of points used:

$$20 \quad f_0 = \frac{1}{2N+1} \quad (31)$$

The wiggles observed on the right-hand side plot of **Fig. 2** (the Gibbs phenomenon) are undesirable if the filter's objective is to remove the highest frequencies from the signal, which is the case for the lidar signal impacted by detection noise. The Gibbs ripples are predicted by the Fourier theory because these digital filters have a finite number of coefficients, the equivalent in the physical domain of truncated Fourier series in the frequency domain. The strength of the frequency approach is to use the Fourier theory, often refined by the concept of windowing, to



minimize the Gibbs ripples. Detailing the underlying theory behind this behavior is beyond the scope of the present paper. Instead, we simply provide below and in the Supplement the most common examples of modifications made to the filter coefficients allowing an optimized design of a noise-reduction filter. More details on filters windows can be found for example in Rabiner and Gold (1975).

5 2.4 Example 2: Low-pass filter and cut-off frequency

If we were to consider an ideal low-pass filter with an infinite number of terms, the theoretical transfer function would have values strictly comprised between 0 and 1 representing the perfect gain of the filter (no ripples). The so-called *transition region* corresponds to the region where we want the transfer function to drop from a value of 1 at lower frequencies to a value of 0 at higher frequencies. The width of the transition region is the *bandwidth*. We can
 10 define the *cut-off frequency* of a low-pass filter as the frequency at which the transfer function equals 0.5. For most low-pass filters this is at the center of the transition region. To design a low-pass filter with the desired cut-off frequency f_c , we start with the initial conditions defining an ideal low-pass filter:

$$\begin{aligned} G(f) &= 1 && \text{for } 0 < |f| < f_c \\ G(f) &= 0 && \text{for } f_c < |f| < 0.5 \end{aligned} \quad (32)$$

15 $G(f) = G(-f)$

Without getting into mathematical details, we find that these conditions are always true for a family of un-truncated Fourier series with the following transfer function:

$$H(f) = 2f_c + 2 \sum_{n=1}^{\infty} \frac{\sin(2\pi n f_c)}{\pi n} \cos(2\pi n f) \quad (33)$$

Since we have to work with a finite number of samples, we truncate the series to a finite number of terms at the
 20 expense of producing Gibbs ripples. The real-world low-pass filter thus created has the following $2N+1$ coefficients and transfer function:

$$c_n = 2f_c \frac{\sin(2\pi n f_c)}{2\pi n f_c} \quad -N \leq n \leq N \quad (34)$$

$$G(f) = H(f) = 2f_c + 2 \sum_{n=1}^N \frac{\sin(2\pi n f_c)}{\pi n} \cos(2\pi n f) \quad (35)$$

An example, for $f_c=0.15$, is provided for reference in **Fig. 3**. The impulse response (left) and gain (right) are shown
 25 for a filter full-width comprised between 3 and 25 points. The first few Gibbs ripples always have the largest amplitude. Using a higher number of terms causes the ripples to be more concentrated near the transition region, and causes higher orders' ripples with a smaller amplitude to occur near the Nyquist frequency.

The gain curves show that the transition region is narrower than that observed for the *smoothing by ns* filters, but the Gibbs ripples appear on both sides of the transition region. Just like for the modified least squares fitting, we can
 30 reduce the magnitude of the Gibbs ripples by modifying the filter coefficients, specifically by applying additional



weights to the filter coefficients, a process called *windowing*. Several examples of smoothing filters using Lanczos, von Hann, Hamming, Blackman, and Kaiser windows are provided for reference in the Supplement.

2.5 Example 3: Central difference derivative filter

The simplest approximation of the derivative of a signal S at altitude $z(k)$ without a phase shift is the so-called 3-point central difference which can be written:

$$S_f(k) = \frac{1}{2}(S(k+1) - S(k-1)) \quad (36)$$

Here we work in units of sampling bins rather than physical units, i.e., we assume the sampling resolution is $\delta z=1$. We recognize the set of coefficients:

$$c_n = \frac{n}{2} \quad -1 \leq n \leq 1 \quad (37)$$

The transfer function, obtained from Eq. (36) is:

$$\lambda(\omega) = \frac{1}{2}[-e^{-i\omega} + 0 + e^{i\omega}] = i \sin \omega \quad (38)$$

Following the notation of Eq. (19) (odd symmetry) and using the values of the coefficients c_n (Eq. (37)), we then compute the gain, i.e., the ratio of the value approximated by the central difference (Eq.

(38)) to the value of the ideal derivative (Eq. (18)) and find:

$$G(f) = \frac{H(f)}{2\pi f} = \frac{\sum_{n=1}^1 \frac{n}{2} \sin(2\pi n f)}{\pi f} = \frac{\sin 2\pi f}{2\pi f} \quad (39)$$

This equation shows that the central difference conserves the slope of the original signal for $f=0$ only, and underestimates this slope for all other frequencies. Figure 4 shows the transfer function H (red solid curve) and gain G (blue solid curve) for the 3-point central differences. Just like for the smoothing filters, we can design derivative low-pass filters that will conserve the slope of the signal for low values of frequency and attenuate the slope (or noise) for higher frequency values. Several examples are given in the Supplement.

3 Review of vertical resolution definitions used by NDACC lidar investigators

The filtering schemes or methods of several NDACC lidar investigators have been reviewed and compared in previous works, for e.g., Beyerle and McDermid (1999) and Godin et al., (1999). These studies concluded that vertical resolution was not consistently reported between the various investigators. Here we briefly review the filtering schemes or methods used by various NDACC lidar investigators, and how vertical resolution is reported in their data files, as of 2011. This review provided critical input to the ISSI Team to determine which definitions of vertical resolution is appropriate for use in a standardized way across the entire network (see section 4).



In the case of the stratospheric ozone differential absorption lidar at Observatoire de Haute-Provence (OHP), a 2nd degree polynomial derivative filter (Savitsky-Golay derivative filter) is used (Godin-Beekmann et al., 2003). Vertical resolution is reported following a definition based on the cut-off frequency of the digital filter.

For the JPL stratospheric ozone and temperature lidars at Table Mountain, CA and Mauna Loa, Hawaii, filtering is done by applying a 4th degree polynomial least-squares fit (Savitsky-Golay derivative filter) to the logarithm of the signals for ozone retrieval. For the temperature profiles, a Kaiser filter is applied to the logarithm of the relative density profile. In both ozone and temperature cases, the cutoff frequency of the filter, reversed to the physical domain, is reported as vertical resolution (Leblanc et al., 2012).

The NASA-GSFC ozone DIAL algorithm (STROZ instrument) (Beyerle and McDermid, 1999) uses a least-squares 4th degree polynomial fit derivative filter (Savitsky-Golay derivative filter). The definition of vertical resolution in the NDACC-archived data files is based on the impulse response of a delta function, by measuring the FWHM of the filter's response. For the temperature retrieval (Gross et al., 1997), the profiles are smoothed using a low-pass filter (Kaiser and Reed, 1977), and a simple ad hoc step function is used to define the values of the vertical resolution.

For the RIVM ozone lidar located in Lauder, New Zealand (Swart et al., 1994), the definition of vertical resolution is based on the width of the fitting window used for the ozone derivation.

The tropospheric ozone DIAL at Reunion Island (France) uses a 2nd degree polynomial least-squares fit (Savitsky-Golay derivative filter) to filter the ozone measurements. The vertical resolution is reported as the cut-off frequency of the corresponding digital filter (same ozone retrieval as for the OHP lidar). For the temperature profiles using the Rayleigh backscatter lidar measurements at Reunion Island, a Hamming filter is applied on the temperature profile. The width of the window used is reported as the vertical resolution.

For climatology studies, the Purple Crow Lidar (PCL) temperature algorithm applies a combination of smoothing by 3s and 5s filters or a Kaiser filter on the temperature profiles (e.g. Argall and Sica, 2007). Similar filters are used in space or time for spectral analysis of atmospheric waves (e.g. Sica and Russell 1999). Filter parameters are reported in the data files locally produced and distributed to the scientific user community. Previously files were distributed to users with the type of filter and full bandwidth of the filter. The variance reduction of the filter is folded into the random uncertainties provided. The product of the data spacing and the filter bandwidth gives the full influence of the filter at each point. With the development of a temperature retrieval algorithm based on an optimal estimation method, vertical resolution of the temperature profile is now available as a function of altitude (Sica and Haefele, 2015).

The ozone DIAL and temperature algorithms of the NDACC lidar in Tsukuba, Japan uses 2nd and 4th degree polynomial least-squares fits (Savitsky-Golay derivative filter). The vertical resolution is calculated from a simulation model that determines the FWHM of the impulse response to an ozone delta function. The FWHM is then mapped as a function of altitude. For temperature a von Hann (or Hanning) window is used on the logarithm of the signal (B. Tatarov, personal communication, 2010).

The IFU tropospheric ozone DIAL algorithm (instrument located in Garmisch-Partenkirchen, Germany) initially used linear and third degree polynomial fits (Kempfer et al., 1994), and then since 1996 a combination of a linear fit



and a Blackman-type window (Eisele and Trickl, 2005; Trickl, 2010). The latter filter has a reasonably high cut-off frequency and do not transmit as much noise as the derivative filters used earlier at IFU (Kempfer et al., 1994). To report vertical resolution in the data files, a Germany-based standard definition of vertical resolution is used, following the Verein Deutscher Ingenieure DIAL guideline (VDI, 1999). This definition is based on the impulse response to a Heaviside step function. The vertical resolution is given as the distance separating the positions of the 25% and 75% in the rise of the response, which is approximately equivalent to the FWHM of the response to a delta function. In the case of the ozone DIAL the vertical resolution of both the Blackman-type filter used and the combined least-squares-derivative plus Blackman filter. A vertical resolution of 19.2 % of the filtering interval was determined, respectively. For small intervals the latter value may change, i.e., the least-squares fit for determining the derivative is executed over just a few data points. For comparison, an arithmetic average yields a vertical resolution of 50 % of the filtering interval.

Having reviewed the vertical resolution definitions and schemes used across NDACC and elsewhere, three definitions or approaches can be clearly identified. The first definition is the number of filter coefficients used, the second definition is based on the cut-off frequency of the filter used, and the third definition is based on the width of the impulse response of the filter used. Those definitions were already mentioned by Beyerle and McDermid (1999), but no decision was made within NDACC to find a standardized approach across the network. The present article and its Supplement show that not all filters have the same properties, and that the characteristics of a filter do not simply depend on the number of coefficients used, but instead on a combination of the number of coefficients and their values. Indeed, **Fig. 5** below shows the gain of several filters having the same number of coefficients (5-pts for the smoothing filters on the left hand plot, and 7-pts for the derivative filters on the right hand plot). It is obvious that, depending on the filter and/or window used, the transition region between pass-band and stop-band is located at very different frequencies. In the examples shown, it is located between $f=0.12$ and $f=0.35$ for smoothing filters, while the derivative filters show considerably more variability.

Finding transition regions at different frequencies means that the smoothing effect of the filters on the signal is different even though the number of coefficients is the same. A vertical resolution definition based on the number of coefficients is therefore not reliable. Instead we need to choose a standardized definition based on objective parameters that are directly related to the effect a filter has on the signal. Two such definitions are proposed thereafter, definitions that are similar or closely related to the two remaining definitions identified in the present section.

4 Proposed standardized vertical resolution definitions for the NDACC lidars

The two definitions proposed here were chosen because they provide a straightforward characterization of the underlying smoothing effect of filters (see **section 2**), and they appear to be already used by a large number of NDACC investigators (see **section 3**). The first definition is based on the width of the impulse response of the filter. The second definition is based on the cut-off frequency of the filter. Further justification for the choice of either definition is provided at the end of the present section.



4.1 Definition based on the FWHM of a finite impulse response

The full-width-at-half-maximum (FWHM) of an impulse response, as introduced in **section 2**, is computed by measuring the distance (in bins) between the two points at which the response magnitude falls below half of its maximum amplitude. The NDACC-lidar-standardized definition of vertical resolution proposed here is computed from the response I_{OUT} of a Kronecker delta function for smoothing filters, and a Heaviside step function for derivative filters. Because of the dynamic range of the lidar signals (or ozone or temperature profiles), we assume that the number of filter coefficients varies with altitude. Therefore, the standardized vertical resolution is estimated separately for each altitude $z(k)$, and the procedure can be summarized as follows:

- 1) Define and/or identify the $2N(k)+1$ filter coefficients $c(k,n)$ used to perform the smoothing or differentiation operation on the lidar signal (or the ozone or temperature profile):

$$S_f(k) = \sum_{n=-N(k)}^{N(k)} c(k,n)S(k+n) \quad \text{for } N(k) < k < nk - N(k) \quad (40)$$

- 2) Construct an impulse function of finite length $2M(k)+1$ to be convolved with the filter coefficients. The value of $M(k)$ is not critical but has to be greater or equal to $N(k)$. For smoothing filters, the impulse function is the Kronecker delta function which can be written:

$$I_{INP}(k,m) = \delta_0(m) \quad \text{with} \quad -M(k) \leq m \leq M(k) \quad \text{and} \quad N(k) \leq M(k) \leq \frac{nk-1}{2} \quad (41)$$

This function equals 1 at the central point ($m=0$) and equals 0 everywhere else. For derivative filters, the impulse function is the Heaviside step function which can be written:

$$I_{INP}(k,m) = H_s(m) \quad \text{with} \quad -M(k) \leq m \leq M(k) \quad \text{and} \quad N(k) \leq M(k) \leq \frac{nk-1}{2} \quad (42)$$

This function equals 0 at all locations below the central point ($m<0$) and equals 1 everywhere else.

- 3) Convolve the filter coefficients with the impulse function in order to obtain the impulse response I_{OUT} :

$$I_{OUT}(k,m) = \sum_{n=-N(k)}^{N(k)} c(k,n)I_{INP}(k,m+n) \quad (43)$$

- 4) Estimate the full width at half-maximum (FWHM) of the impulse response I_{OUT} , by measuring the distance Δm_{IR} , in bins, between the two points (located on each side of the central bin) where the response magnitude falls below half of the maximum amplitude:

$$I_{OUT}(k,m_1(k)) = 0.5 \max(I_{OUT}(k,m_i)) \quad \text{for all } -M(k) \leq m_i \leq 0$$

$$I_{OUT}(k,m_2(k)) = 0.5 \max(I_{OUT}(k,m_i)) \quad \text{for all } 0 \leq m_i \leq M(k) \quad (44)$$

$$\Delta m_{IR}(k) = |m_1(k) - m_2(k)| \quad (45)$$

- For a successful identification of the FWHM, the impulse response should have only two points where its value falls below half of its maximum amplitude, which is normally the case for all smoothing and derivative filters used within their prescribed domain of validity (see examples in section 2 and in the Supplement). In the event that more than



two points exist, the two points farthest from the central bin should be chosen in order to yield the most conservative estimate of vertical resolution.

5) Compute the standardized vertical definition Δz_{IR} as the product of the lidar sampling resolution δz and the estimated FWHM:

$$5 \quad \Delta z_{IR}(k) = \delta z \Delta m_{IR}(k) \quad (46)$$

Figure 6 summarizes the estimation procedure just described. The unsmoothed signal yields a FWHM of 1 bin. This result is easily derived by considering null coefficients everywhere except at the central point ($m=0$), where the coefficient equals 1. The intercept theorem within the triangles formed by the impulse response at the central point and its two adjacent points ($m=-1$ and $m=1$) yields a FWHM of 1 bin, and the standardized vertical resolution using the present impulse response-based definition will always be greater or equal to the sampling resolution:

$$10 \quad \Delta z_{IR}(k) \geq \delta z \quad \text{for all } k \quad (47)$$

When several filters are applied successively to the signal, the response of the filter must be computed each time a filtering operation occurs, and vertical resolution needs to be computed only after the last filtering occurrence. The process can be summarized as follows: a first impulse response is computed with the first filtering operation. If no further filtering occurs, the impulse response is used to determine the FWHM and vertical resolution. If a second filtering operation occurs, the impulse response is used as input signal, and a second response is computed from the convolution of this input signal with the coefficients of the second filter. If no further filtering occurs, the second response is used to determine the FWHM and vertical resolution. If a third filtering operation occurs, the response output from the second convolution is used as input signal of the third convolution, and so on until no more filtering occurs. Vertical resolution is always computed from the final output response, i.e., after the final filtering operation. The schematics shown in **Fig. 7** summarize the procedure.

4.2 Definition based on the cut-off frequency of digital filters

The cut-off frequency of digital filters is defined as the frequency at which the value of the filter's gain is 0.5, typically located at the center of the transition region between the passband and the stopband (see **section 2**). The NDACC-lidar-standardized definition proposed here is computed from the cut-off frequency f_c , which is determined from the gain of the filter obtained by applying a Laplace Transform to the coefficients of the filter used. Once again, because of the dynamic range of the lidar signals, filtering a lidar signal (or ozone/temperature profile) typically requires to use a number of filter coefficients varying with altitude. Starting with a lidar signal (or ozone or temperature profile) S made of nk equally-spaced elements in the vertical dimension, the standardized vertical resolution is estimated separately for each altitude $z(k)$, and the procedure can be summarized as follows for each altitude considered:

1) Define and/or identify the $2N(k)+1$ filter coefficients $c(k,n)$ used to perform the smoothing or differentiation operation on the lidar signal (or on the ozone or temperature profile) at altitude:

$$S_f(k) = \sum_{n=-N(k)}^{N(k)} c(k,n)S(k+n) \quad \text{for } N(k) < k < nk - N(k) \quad (48)$$



2) Apply the Laplace Transform to the coefficients to determine the filter's transfer function and gain. For non-derivative smoothing filters, the coefficients have even symmetry, i.e., $c(k,n)=c(k,-n)$, and the gain is written:

$$G(k, f) = H(k, f) = c(k,0) + 2 \sum_{n=1}^{N(k)} c(k, n) \cos(2\pi n f) \quad 0 < f < 0.5 \quad (49)$$

For derivative filters, the coefficients have odd symmetry, i.e., $c(k,n)=-c(k,-n)$, and if δz is the sampling resolution, the gain can be written:

$$G(k, f) = \frac{H(k, f)}{2\pi f} = 2 \sum_{n=1}^{N(k)} c(k, n) \frac{\sin(2\pi n f)}{2\pi f} \quad 0 < f < 0.5 \quad (50)$$

For a successful cut-off frequency estimation process, the gain must be computed with normalized coefficients c_n , that is, the coefficients must meet the following normalization condition:

$$\sum_{n=-N(k)}^{N(k)} c(k, n) = 1 \quad \text{for smoothing filters}$$

$$2 \sum_{n=1}^{N(k)} n c(k, n) = 1 \quad \text{for derivative filters} \quad (51)$$

3) Estimate the cut-off frequency, i.e., the frequency f_C at which the gain equals 0.5:

$$G(k, f_C(k)) = 0.5 \quad 0 < f_C(k) \leq 0.5 \quad (52)$$

For a successful identification, the gain should have only one crossing with the 0.5-line. This is normally the case for all smoothing and derivative filters used within their prescribed domain of validity. In the event that several crossings exist, the frequency closest to zero should be chosen to ensure that the most conservative estimate of vertical resolution is retained.

4) Calculate the cut-off length Δm_{FC} (unit: bins), i.e., the inverse of the frequency f_C normalized to the sampling width:

$$\Delta m_{FC}(k) = \frac{1}{2f_C(k)} \quad (53)$$

5) Compute the standardized vertical definition Δz_{FC} as the product of the lidar sampling resolution δz and the cut-off length Δm_{FC} at that altitude:

$$\Delta z_{FC}(k) = \delta z \Delta m_{FC}(k) = \frac{\delta z}{2f_C(k)} \quad (54)$$

Figure 8 summarizes the estimation procedure just described. The factor of 2 present in the denominator of **Eq. (53)** is usually not used in spectral analysis, when it is normally assumed that the minimum vertical scale that can be resolved by the instrument is twice the sampling resolution (Nyquist criterion). However, it is included here in order to harmonize the numerical values with the values computed using the impulse response definition. Using the present proposed definition, an unsmoothed signal yields a vertical resolution of δz and the standardized vertical resolution will always be at least equal to the sampling resolution:



$$\Delta z_{FC}(k) \geq \delta z \quad \text{for all } k \quad (55)$$

When several filters are applied successively to the signal, the transfer function must be computed each time a filtering operation occurs, but vertical resolution needs to be computed only after the last filtering occurrence. The process can be summarized as follows: a first transfer function (or gain) is computed with the first filtering operation. When the second filtering operation occurs, the gain computed using the coefficients of the second operation is multiplied by the gain computed during the first filtering operation. If no further filtering occurs, the result of this product is the gain that should be used to determine the cut-off frequency and vertical resolution. If a third filtering operation occurs, the product of the first and second gain must be multiplied by the third gain, and so on until no more filtering occurs. When the final filtering operation is reached, vertical resolution can be computed from the final output gain. The schematics shown in **Fig. 9** summarize the procedure.

4.3 Comparison between the impulse response-based (IR) and cut-off frequency-based (CF) definitions

In **sections 4.1 and 4.2**, we showed that, when using the proposed definitions based on impulse response and cut-off frequency, the standardized vertical resolution of an unsmoothed lidar signal (or profile) is equal to the lidar sampling resolution. However this equality between the two definitions is not perfect for all filters. Here, we show that for most filters, there is a well-defined proportionality relation between the two definitions, but we also show that the proportionality factor depends on the type of filter used. In the rest of this section, for convenience we will work with vertical resolutions normalized by the sampling resolution (unit: bins). The results are therefore shown as cut-off width Δm_{FC} and impulse response FWHM Δm_{IR} instead of Δz_{FC} and Δz_{IR} respectively, which is equivalent to assuming $\delta z=1$.

Figure 10 shows, for the smoothing filters introduced in **section 2** and in the **Supplement**, the correspondence between the standardized vertical resolutions (in bins) computed using the cut-off frequency and using the impulse response, for full-widths comprised between 3 and 25 points. The black solid circle at coordinate (1,1) indicates the vertical resolution for the unsmoothed signal (or profile). The grey horizontal and vertical dash-dotted lines indicate the highest possible vertical resolutions for the impulse response-based and cut-off frequency-based definitions respectively. The grey dotted straight lines indicate the result of the linear regression fits between the two definitions, and the numbers at their extremity are the values of the slope for three of the four types of filters used. There is no proportionality between the two definitions for the low-pass filters (diamonds) because the cut-off frequency is prescribed for this type of filter. Note that the factors of 1.2 and 1.39 do not correspond to the ratio of 1.0 that is assumed for the unsmoothed signal. Very similar conclusions can be drawn for the derivative filters, as demonstrated by **Fig. 11** (which is similar to **Fig. 10** but for the derivative filters introduced in **section 2** and in the **Supplement**).

Figure 12 is similar to **Fig. 10**, but this time after the filters were convolved with the windows introduced in the **Supplement**. The windows change the proportionality constant between the two definitions, but this constant appears to be approximately the same for a given window, specifically around 1.04 for Lanczos, 1.0 for von Hann, 0.92 for Blackman, and 1.0 for Kaiser (50-dB). **Table 1** summarizes the proportionality constants for all filters and all windows introduced in **section 2** and in the **Supplement**.



Figure 13 shows, for the filters introduced in **section 2** and in the **Supplement**, the correspondence between the two proposed standardized vertical resolutions (in bins) and the number of filter coefficients used (full-widths comprised between 3 and 25 points). The dashed grey line represents unity slope (i.e., 1 bin for 1 filter coefficient), and the numbers at the end of the red and blue dotted straight lines indicate the slope of the linear fit applied to the paired points for each definition. As expected for a boxcar average, the impulse response-based definition yields a vertical resolution (in bins) that is equal to the number of terms used (see **Fig. 2**). This is a particular case for which reporting vertical resolution using the number of filter terms yields a result identical to the impulse response-based standardized definition. Note that for low-pass filters with a prescribed cut-off frequency, the vertical resolution does not depend at all on the number of filter terms used (right hand plot).

Figure 14 is similar to **Fig. 13**, this time after convolution by a von Hann window. Except for the low-pass filter, there is a factor of approximately 2 between the number of terms used by the filter and the vertical resolution for both definitions. **Figure 15** is similar to **Fig. 13**, but for three selected derivative filters.

The factors between the vertical resolutions (in bins) and the number of filter coefficients are compiled in **Table 2** and **Table 3** for the cut-off frequency-based and the impulse response-based definition respectively.

In this section, it was shown that each recommended definition of vertical resolution yields its own numerical values, i.e., for a same set of filter coefficients, the reported standardized vertical resolution will likely have two different numerical values, depending on the definition used. Unfortunately, there is no unique proportionality factor between the two definitions that could be used for all digital filters in order to obtain a “unified” homogenous definition yielding identical values. However, after reviewing this homogeneity problem, the ISSI Team concluded that both definitions should still be recommended because the computed values remain close, specifically within 10% if using windows and within 20% if not using windows, and because each definition is indeed useful for specific applications. For example, the cut-off frequency-based definition is particularly useful for gravity waves studies from lidar temperature measurements, because it can provide, through the transfer function, spectral information that can help interpreting quantitative findings on the amplitude and wavelength of lidar-observed waves. This type of information is not available when using the impulse response-based definition. On the other hand, the impulse response-based definition is widely used in atmospheric remote sensing, and provides information in the physical domain similar to that provided through the averaging kernels of optimal estimation methods used for passive measurements (e.g., microwave radiometer measurement of ozone or temperature).

4.4 Additional recommendations to ensure full traceability

When archiving the ozone or temperature profiles, reporting values of vertical resolution using a standardized definition such as Δz_{FC} or Δz_{IR} constitutes an important improvement from other, non-standardized, methods such as the number of points used by the filter. However, using one standardized definition or even both standardized definitions proposed here, still does not characterize the complete smoothing effect of the filter on the signal. For full traceability, it is necessary to provide for each altitude point, either the set of filter coefficients used (for one-time smoothing cases) or to provide the complete transfer function or impulse response. This information can be



critical when comparing the lidar profiles with profiles from other instruments, or when working with averaging kernels used for other measurements.

If the data provider chooses to report standardized vertical resolution information based on the impulse response definition, the complete vertical resolution information should include:

- 5 1) A vector Δz_{IR} of length nk containing the standardized vertical resolution values at each altitude, as proposed in **section 4.2**
- 2) A two-dimensional array of size $nk \times nm$ containing the full impulse response used to estimate the FWHM ($nm=2M+1$ is the full-length of the impulse function convolved with the filter coefficients, and a recommended value is $nm=nk$)
- 10 3) A vector m of length nm containing the distance (in bins) from the central bin at which the response is reported
- 4) Meta data information describing clearly the nature of the reported vectors and arrays

If the data provider chooses to report standardized vertical resolution information based on the cut-off frequency definition, the complete vertical resolution information should therefore include:

- 15 1) A vector Δz_{FC} of length nk containing the standardized vertical resolution values at each altitude, as proposed in **section 4.1**
- 2) A two-dimensional array of size $nk \times nf$ containing the gain used to estimate the cut-off frequency (nf is the number of frequencies used when applying a Laplace transform to the filter coefficients, and a recommended value is $nf=nk$)
- 20 3) A vector f of length nf containing the values of frequency at which the gain is reported
- 4) Meta data information describing clearly the nature of the reported vertical resolution vector, frequency vector, and two-dimensional gain array

If the data provider chooses to report standardized vertical resolution based on both the impulse response definition and the cut-off frequency definition, the complete vertical resolution information should include:

- 25 1) A vector Δz_{IR} of length nk containing the standardized vertical resolution values at each altitude, as proposed in **section 4.2**
- 2) A two-dimensional array of size $nk \times nm$ containing the full impulse response used to estimate the FWHM ($nm=2M+1$ is the full-length of the impulse function convolved with the filter coefficients, and a recommended value is $nm=nk$)
- 30 3) A vector m of length nm containing the distance (in bins) from the central bin at which the response is reported
- 4) A vector Δz_{FC} of length nk containing the standardized vertical resolution values at each altitude, as proposed in **section 4.1**
- 5) A two-dimensional array of size $nk \times nf$ containing the gain used to estimate the cut-off frequency (nf is the number of frequencies used when applying a Laplace transform to the filter coefficients, and a recommended value is $nf=nk$)
- 35 6) A vector f of length nf containing the values of frequency at which the gain is reported



- 7) Meta data information describing clearly the nature of all reported vectors and arrays

4.5 Practical implementation within NDACC

Numerical tools were developed and provided to the NDACC PIs in order to facilitate the implementation of the network-wide use of the proposed standardized definitions. These tools consist of easy-to-use plug-in routines written in IDL, MATLAB and FORTRAN, which convert a set of filter coefficients into the needed standardized values of vertical resolution following one or the other proposed definitions. The tools are written in such a way that they can be called in a lidar data processing algorithm each time a smoothing and/or differentiating operation occurs. The routines can handle multiple smoothing and/or differentiating operations applied successively throughout the lidar data processing chain, as described in **sections 4.1** and **4.2**. The routines are available upon request to thierry.leblanc@jpl.nasa.gov.

The routine “NDACC_ResolIR” computes vertical resolution values with a definition based on the FWHM of the filter’s impulse response. When the routine is called for the first time in the data processing chain, the sampling resolution and the coefficients of the filter are the only input parameters of the routine. The routine convolves the coefficients with an impulse (delta function for smoothing filters and Heaviside function for derivative filters) to obtain the filter’s impulse response, and then identifies the full-width at half-maximum (FWHM) of this response. The response and the value of vertical resolution are the output parameters of the routine. The product of the response full width by the sampling resolution is performed inside the routine. When a second call to the routine occurs (second smoothing occurrence), the vertical resolution output from the first call is no longer used. Instead, the response output from the first call is used as input parameter for the second call, together with the sampling resolution and the coefficients of the second filter. The input response is convoluted with the coefficients of the second filter to obtain a second response. The routine identifies the FWHM of this new response. Once again the vertical resolution is computed inside the routine by calculating the product of the new FWHM and the sampling resolution. The new response and the new vertical resolution are the output parameters of the routine after the second call. The procedure is repeated as many times as needed, i.e., as many times as a smoothing or differentiation operation occurs.

The routine “NDACC_ResolDF” computes vertical resolution values with a definition based on the cut-off frequency of a digital filter. When the routine is called for the first time in the data processing chain, the sampling resolution and the coefficients of the filter are the only input parameters of the routine. The routine applies a Laplace transform to the coefficients to obtain the filter’s gain, and then identifies the cut-off frequency. The inverse of the doubled cut-off frequency is multiplied by the sampling resolution to obtain the vertical resolution. The gain and the vertical resolution are the output parameters of the routine. When a second call to the routine occurs (i.e., a second smoothing operation occurs), the cut-off width output from the first call is not used anymore. Instead, the gain output from the first call is used as input parameter for the second call, together with the sampling resolution and the coefficients of the second filter. The product of the input gain and gain computed from the second filter is the new gain from which the routine identifies the cut-off frequency. A new vertical resolution is obtained by multiplying the inverse of the newly-computed doubled cut-off frequency by the sampling resolution. The new gain and the new



vertical resolution are the output parameters of the routine after the second call. The procedure is repeated as many times as needed, i.e., as many times as a smoothing or differentiation operation occurs.

The standardization tools became available in summer 2011. They were distributed to several members of the ISSI Team for testing and validation. Using simulated lidar signals and a series of Monte-Carlo experiments, their implementation was validated for several NDACC ozone and temperature lidar algorithms. Several examples of this validation are provided in the ISSI Team Report (Leblanc et al., 2016a). Ideally, an NDACC-wide implementation should follow. The implementation will not be considered complete until the vertical resolution outputs of all contributing data processing software have been quantified and validated following the same procedure as that described in Leblanc et al. (2016a).

10 5. Summary and conclusion

Over the years, NDACC lidar PIs have been providing temperature and ozone profiles using a wide range of vertical resolution schemes and values, and these values were reported using different definitions. In the present work, we did not recommend using a specific vertical resolution scheme, but instead we recommended using one or two standardized definitions of vertical resolution that can unequivocally describe the impact of any vertical resolution scheme used across the network. The proposed approach was designed so that the standardized definitions can be implemented easily and consistently by all lidar investigators (e.g., NDACC, TOLNet, etc.). Though the recommendations apply to the retrieval of ozone by the differential absorption technique and temperature by the density integration technique, they can likewise apply to the retrieval of other NDACC species such as water vapor (Raman and differential absorption techniques), temperature (rotational Raman technique), and aerosol backscatter ratio at the exception of the Optimal Estimation Method (OEM) for the retrieval of temperature recently proposed by Sica and Haeferle (2015), for which vertical resolution is determined from the FWHM of the OEM's averaging kernels.

The coefficients of the filter used in the vertical smoothing operation are chosen by the lidar investigator, and therefore constitute the key information for the derivation of vertical resolution using a standardized definition. The first “standardized” definition recommended for use in the NDACC ozone and temperature lidar algorithms is based on the width of the response to a Finite Impulse-type perturbation. The response is computed by convolving the filter coefficients with an impulse function, namely, a Kronecker Delta function for smoothing filters, and a Heaviside Step function for derivative filters. Once the response has been computed, the standardized definition of vertical resolution proposed by the ISSI Team is given by $\Delta z = \delta z * H_{FWHM}$, where δz is the lidar's sampling resolution and H_{FWHM} is the full-width at half-maximum (FWHM) of the response, measured in sampling intervals. Following this definition, an unsmoothed signal yields the best possible vertical resolution $\Delta z = \delta z$ (one sampling bin). This definition was recommended by the ISSI Team because it is already widely used within the NDACC community, and it has many points of commonality with the averaging kernels reported for the retrieval of atmospheric species using passive techniques and optimal estimation methods. This definition also allows multiple smoothing occurrences to be treated analytically in a simple and exact manner.



The other recommended definition relates to digital filtering theory. After applying a Laplace Transform to a set of filter coefficients, we can derive the filter transfer function and gain, which characterize the effect of the filter on the signal in the frequency-domain. A cut-off frequency value f_c can be defined as the frequency at which the gain equals 0.5, and vertical resolution can then be defined by the relation $\Delta z = \delta z / (2f_c)$. Unlike common practice in the field of spectral analysis, a factor $2f_c$ instead of f_c was indeed proposed here to yield values conveniently close to the values obtained with the impulse response definition. The present definition therefore yields vertical resolution values expressed as multiples of sampling intervals rather than multiples of Nyquist intervals, and an unsmoothed signal yields the best possible vertical resolution $\Delta z = \delta z$ (one sampling interval), corresponding in the frequency domain, to twice the Nyquist frequency. Like in the impulse response case, the values of vertical resolution computed for multiple, successive smoothing operations is conceptually, theoretically and numerically exact.

The ISSI-Team developed numerical tools to support the implementation of these definitions across the NDACC lidar groups. The tools consist of ready-to-use “plug-in” routines written in IDL, FORTRAN and MATLAB that can be inserted into any lidar data processing software each time a smoothing operation occurs in their data processing chain. The routine’s input parameters are the lidar sampling resolution and the coefficients of the smoothing filter locally applied, and the output parameter is the vertical resolution following the impulse response-based standardized definition, or the cut-off frequency-based standardized definition. When multiple smoothing operations occur within the same data processing chain, the plug-in routines must be called each time smoothing occurs, but the final vertical resolution to be reported is computed only at the final occurrence. The values output by the routines after the last call are reported in the lidar data files together with the ozone or temperature profiles. These standardized values of vertical resolution are theoretically and numerically exact, even after multiple filtering occurrences. Using simulated lidar signals and a series of Monte-Carlo experiments, their implementation was validated for several NDACC ozone and temperature lidar algorithms. Examples of this validation are provided in the ISSI Team Report (Leblanc et al., 2016a).

In our two companion papers (Leblanc et al., 2016b; 2016c), the ISSI Team provided recommendations on the standardized treatment of uncertainty for the NDACC ozone and temperature lidars (Part 2 and Part 3 respectively). It is anticipated that the widespread use of the standardized definitions and approaches proposed in our three companion papers will significantly improve the interpretation of atmospheric measurements, whether these measurements are made for validation purposes (e.g., comparison of correlative measurements) or scientific purposes (e.g., studies of vertical structures observed in the measured profiles). However, an accurate timeline for the completion of this implementation is difficult to define, because the implementation process involves a large number of lidar groups, within and beyond NDACC.

Acknowledgements

This work was initiated in response to the 2010 Call for International Teams of Experts in Earth and Space Science by the International Space Science Institute (ISSI) in Bern, Switzerland. It could not have been performed without the travel and logistical support of ISSI. Part of the work described in this report was carried out at the Jet Propulsion Laboratory, California Institute of Technology, under agreements with the National Aeronautics and



Space Administration. Part of this work was carried out in support of the VALID Project. RJS would like to acknowledge the support of the Canadian National Sciences and Engineering Research Council for support of The University of Western Ontario lidar work.

References

- 5 Argall, P. S., and Sica, R. J.: A comparison of Rayleigh and sodium lidar temperature climatologies, *Ann. Geophys.*, 25, 27-35, 10.5194/angeo-25-27-2007, 2007.
- Arshinov, Y. F., Bobrovnikov, S. M., Zuev, V. E., and Mitev, V. M.: Atmospheric-temperature measurements using a pure rotational Raman lidar, *Appl. Opt.*, 22, 2984-2990, 1983.
- Beyerle, G., and McDermid, I. S.: Altitude Range Resolution of Differential Absorption Lidar Ozone Profiles, *Appl. Opt.*, 38, 924-927, 1999.
- 10 Birge, R. T., and Weinberg, J. W.: Least-Squares' Fitting of Data by Means of Polynomials, *Rev. Mod. Phys.*, 19, 298, 1947.
- D'Amico, G., Amodeo, A., Baars, H., Biniotoglou, I., Freudenthaler, V., Mattis, I., Wandinger, U., and Pappalardo, G.: EARLINET Single Calculus Chain – overview on methodology and strategy, *Atmos. Meas. Tech.*, 8, 4891-4916, 10.5194/amt-8-4891-2015, 2015.
- 15 Eisele, H., and Trickl, T.: Improvements of the aerosol algorithm in ozone lidar data processing by use of evolutionary strategies, *Appl. Opt.*, 44(13), 2638-2651, 2005.
- Godin, S., Carswell, A. I., Donovan, D. P., Claude, H., Steinbrecht, W., McDermid, I. S., McGee, T. J., Gross, M. R., Nakane, H., Swart, D. P. J., Bergwerff, H. B., Uchino, O., von der Gathen, P., and Neuber, R.: Ozone
- 20 Differential Absorption Lidar Algorithm Intercomparison, *Appl. Opt.*, 38(30), 6225-6236, 1999.
- Godin-Beekmann, S., Porteneuve, J., and Garnier, A.: Systematic DIAL lidar monitoring of the stratospheric ozone vertical distribution at Observatoire de Haute-Provence (43.92 degrees N, 5.71 degrees E), *J. Environ. Monit.*, 5, 57-67, 10.1039/b205880d, 2003.
- Gross, M. R., McGee, T. J., Ferrare, R. A., Singh, U. N., and Kimvilakani, P.: Temperature measurements made
- 25 with a combined Rayleigh-Mie and Raman lidar, *Appl. Opt.*, 36, 5987-5995, 1997.
- Hamming, R. W.: *Digital Filters*, Third Edition ed., Prentice Hall, Englewood Cliffs, New Jersey, 1989.
- Hauchecorne, A., and Chanin, M. L.: Density and temperature profiles obtained by lidar between 35-km and 70-km, *Geophys. Res. Lett.*, 7, 565-568, 1980.
- Iarlori, M., Madonna, F., Rizi, V., Trickl, T., and Amodeo, A.: Effective resolution concepts for lidar observations,
- 30 *Atmos. Meas. Tech.*, 8, 5157-5176, 10.5194/amt-8-5157-2015, 2015.
- Kaiser, J. F., and Reed, W. A.: Data smoothing using low-pass digital-filters, *Rev. Sci. Instr.*, 48, 1447-1457, 1977.
- Kempfer, U., Carnuth, W., Lotz, R., and Trickl, T.: A wide-range ultraviolet lidar system for tropospheric ozone measurements: Development and application, *Rev. Sci. Instr.*, 65, 3145-3164, 10.1063/1.1144769, 1994.
- Knuth, D. E.: Johann Faulhaber and sums of powers, *Math. Comp.*, 61, 277-294, 10.2307/2152953, 1993.
- 35 Leblanc, T., McDermid, I. S., Hauchecorne, A., and Keckhut, P.: Evaluation of optimization of lidar temperature analysis algorithms using simulated data, *J. Geophys. Res.*, 103, 6177-6187, 1998.



- Leblanc, T., McDermid, I. S., and Walsh, T. D.: Ground-based water vapor raman lidar measurements up to the upper troposphere and lower stratosphere for long-term monitoring, *Atmos. Meas. Tech.*, 5, 17-36, 10.5194/amt-5-17-2012, 2012.
- 5 Leblanc, T., Sica R., van Gijssel, J. A. E., Godin-Beekmann, S., Haefele, A., Trickl, T., Payen, G., and Liberti, G.: Standardized definition and reporting of vertical resolution and uncertainty in the NDACC lidar ozone and temperature algorithms, ISSI Team on NDACC Lidar Algorithms Report, available for download at http://www.issibern.ch/teams/ndacc/ISSI_Team_Report.htm, 2016a.
- 10 Leblanc, T., Sica R., van Gijssel, J. A. E., Godin-Beekmann, S., Haefele, A., Trickl, T., Payen, G., and Liberti, G.: Proposed standardized definitions for vertical resolution and uncertainty in the NDACC lidar ozone and temperature algorithms. Part 2: Ozone DIAL uncertainty budget, *Atmos. Meas. Tech.*, submitted, this issue, 2016b.
- 15 Leblanc, T., Sica R., van Gijssel, J. A. E., Godin-Beekmann, S., Haefele, A., Trickl, T., Payen, G., and Liberti, G.: Proposed standardized definitions for vertical resolution and uncertainty in the NDACC lidar ozone and temperature algorithms. Part 3: Temperature uncertainty budget, *Atmos. Meas. Tech.*, submitted, this issue, 2016c.
- Mégie, G., Allain, J. Y., Chanin, M. L., and Blamont, J. E.: Vertical Profile of Stratospheric Ozone by Lidar Sounding from Ground, *Nature*, 270, 329-331, 1977.
- Rabiner, L. R., and Gold, B.: *Theory and Application of Digital Signal Processing*, Prentice-Hall, Inc., Englewood Cliffs, N.J., 1975.
- 20 Savitzky, A., and Golay, M. J. E.: Smoothing and differentiation of data by simplified least squares procedures, *Anal. Chem.*, 36, 1627-1639, 1964.
- Sica, R. J., and Russell, A. T.: Measurements of the effects of gravity waves in the middle atmosphere using parametric models of density fluctuations. Part I: Vertical wavenumber and temporal spectra, *J. Atmos. Sci.*, 56, 1308-1329, 1999.
- 25 Sica, R. J., and Haefele, A.: Retrieval of temperature from a multiple-channel Rayleigh-scatter lidar using an optimal estimation method, *Appl. Opt.*, 54(8), 1872-1889, 10.1364/ao.54.001872, 2015
- Steinier, J., Termonia, Y., and Deltour, J.: Smoothing and differentiation of data by simplified least square procedure, *Anal. Chem.*, 44, 1906-1909, 10.1021/ac60319a045, 1972.
- 30 Swart, D. P. J., Apituley, A., Spakman, J., Visser, E. P., and Bergwerff, H. B.: RIVMs tropospheric and stratospheric ozone lidars for European and global monitoring networks, *Proceedings of the 17th International Laser Radar Conference*, Laser Radar Society of Japan, Sendai, Japan, 1994, 405-408, 1994.
- Trickl, T.: Tropospheric trace-gas measurements with the differential-absorption lidar technique, in: *Recent Advances in Atmospheric Lidars*, L. Fiorani, V. Mitev, Eds., INOE Publishing House, Bucharest (Romania), Series on Optoelectronic Materials and Devices, Vol. 7, ISSN 1584-5508, ISSN 978-973-88109-6-9, 87-147, 35 2010; revised version available at <http://www.trickl.de/DIAL.PDF>.
- VDI Guideline 4210, Verein Deutscher Ingenieure, Düsseldorf, Germany, 1999.



Table 1: Proportionality factor between the impulse response-based and the cut-off frequency-based definitions of vertical resolution for the filters and windows introduced in section 2 and in the Supplement

Ratio $\Delta z_{IR}/\Delta z_{FC}$	LS and MLS deg. 0-1	LS deg. 2-3	LS deriv. deg. 1-2	LS deriv. deg. 3-4	LS derive. deg. 5-6
No window	1.20	1.39	1.12	1.23	1.24
w/ Lanczos window	1.03	1.04	0.98	0.97	1.07
w/ von Hann window	1.00	0.98	/	/	/
w/ Blackman window	0.92	0.94	0.92	0.92	0.95
w/ Kaiser 50-dB window	0.98	1.02	0.97	0.98	1.05

5

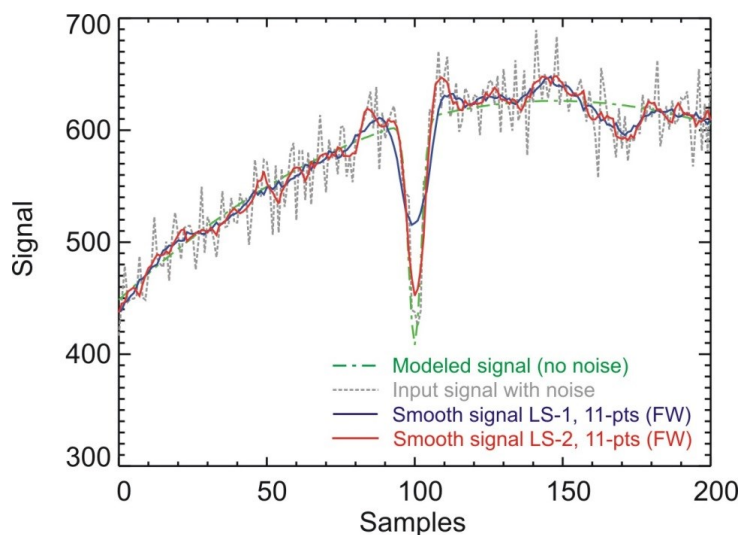
Table 2: Proportionality factor between the number of filter coefficients (full-width) and vertical resolution based on cut-off frequency (in bins) for the filters and windows introduced in section 2 and in the Supplement

Ratio $\Delta m_{FC}/(2N+1)$	LS and MLS deg. 0-1	LS deg. 2-3	LS deriv. deg. 1-2	LS deriv. deg. 3-4	LS derive. deg. 5-6
No window	0.83	0.40	0.63	0.34	0.26
w/ Lanczos window	0.58	0.42	0.51	0.40	0.30
w/ von Hann window	0.50	0.43	/	/	/
w/ Blackman window	0.43	0.36	0.40	0.35	0.30
w/ Kaiser 50-dB window	0.57	0.41	0.50	0.39	0.30

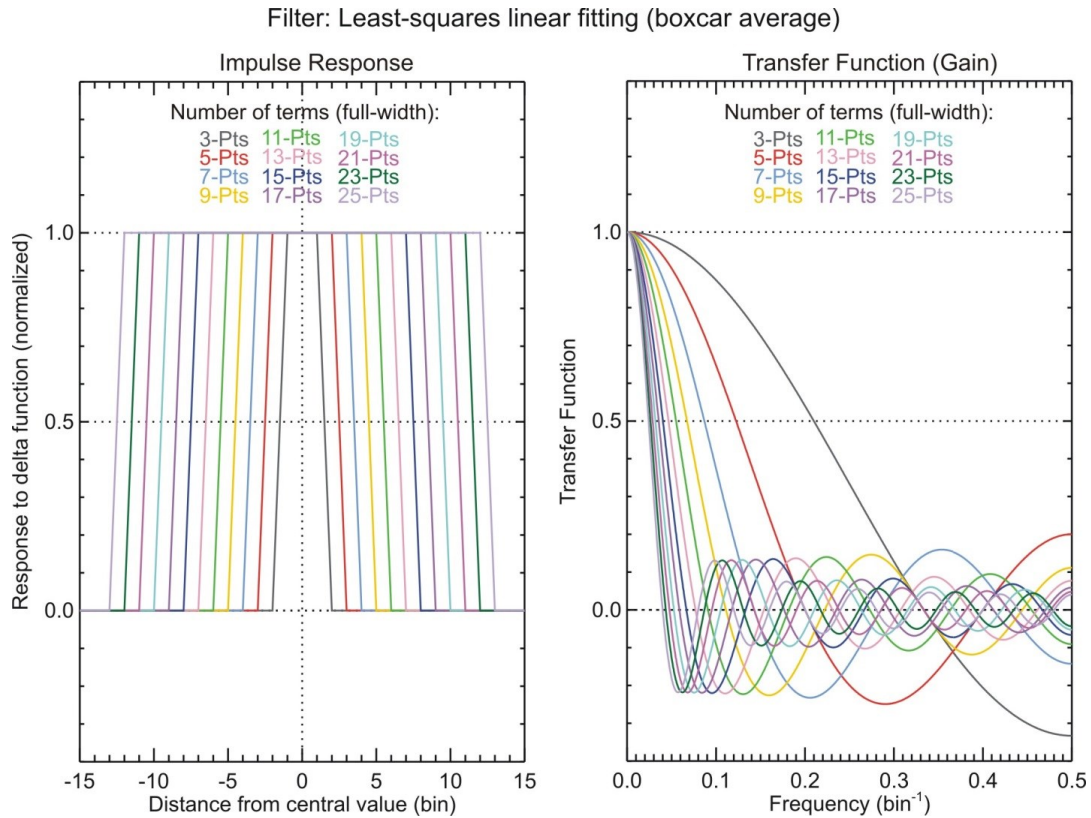
10

Table 3: Proportionality factor between the number of filter coefficients (full-width) and vertical resolution based on impulse response FWHM (in bins) for the filters and windows introduced in section 2 and in the Supplement

Ratio $\Delta m_{IR}/(2N+1)$	LS and MLS deg. 0-1	LS deg. 2-3	LS deriv. deg. 1-2	LS deriv. deg. 3-4	LS derive. deg. 5-6
No window	1.00	0.56	0.71	0.42	0.33
w/ Lanczos window	0.60	0.43	0.50	0.38	0.32
w/ von Hann window	0.50	0.39	/	/	/
w/ Blackman window	0.41	0.34	0.37	0.31	0.29
w/ Kaiser 50-dB window	0.56	0.42	0.49	0.37	0.31



5 Figure 1: Example of the differing impact of two smoothing filters of identical number of terms ($2N+1=11$). The green dot-dash curve is the modelled signal (with no noise), the grey dotted curve is the modelled input signal containing Poisson noise, the blue and red curves are the smoothed signal using a 11-pts boxcar average (LS-1) and the Least - squares fitting method with a polynomial of degree 2 (LS-2), respectively



5 **Figure 2: Impulse response (left) and gain (right) for a digital filter equivalent to fitting an unsmoothed signal with a polynomial of degree 1 or 2 using the least-squares method over an interval comprising $2N+1$ points (full width). Full widths represented in this figure range from 3 to 25 points. This least-squares filtering procedure is equivalent to a running average over $2N+1$ points (full width) as well as smoothing by $(2N+1)s$**

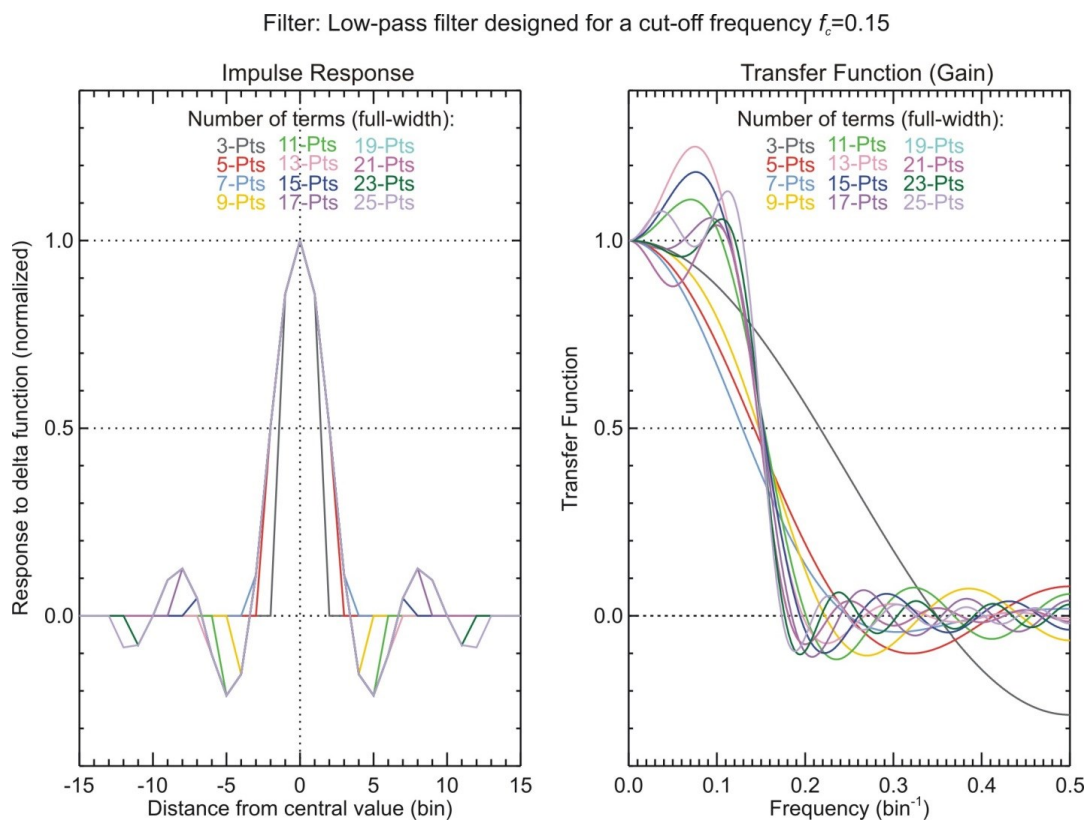


Figure 3: Impulse response and gain of low-pass filters using $2N+1$ coefficients (full width), and designed to have a cut-off frequency $f_c=0.15$. Full widths range from 3 to 25 points.

5

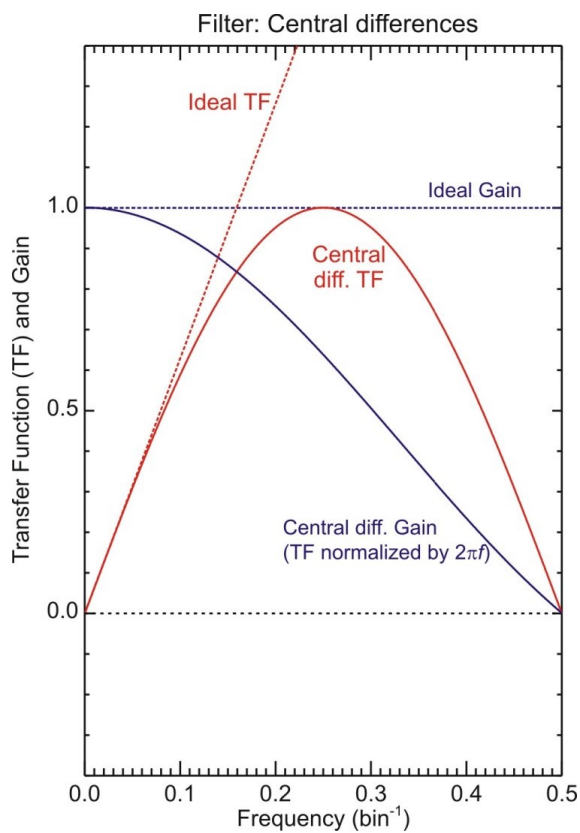
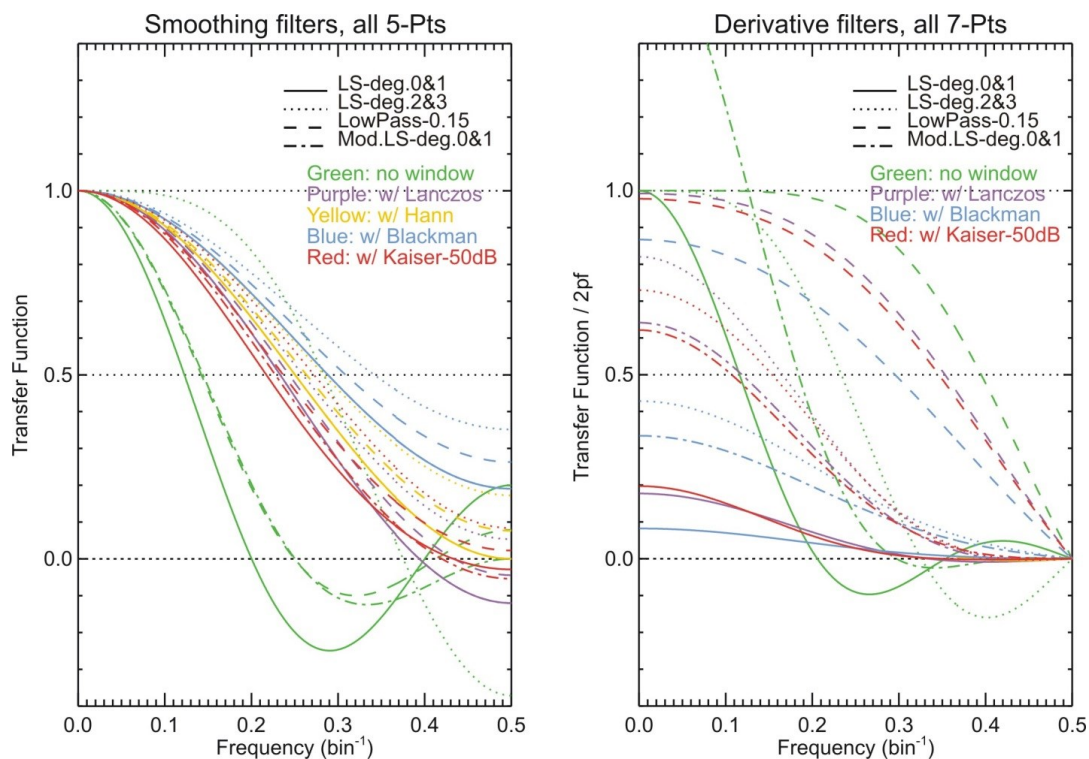


Figure 4: Transfer function (TF) and gain of the central difference digital filter. The gain (blue curve) is the transfer function (red curve) normalized by $2\pi f$, which is the real part of the ideal differentiator $i\omega$

5



5 **Figure 5: Transfer function (gain) of several smoothing (left) and derivative (right) filters, all having the exact same number of coefficients $2N+1$ (5-pts full-width for the smoothing filters and 7-pts full-width for the derivative filters)**

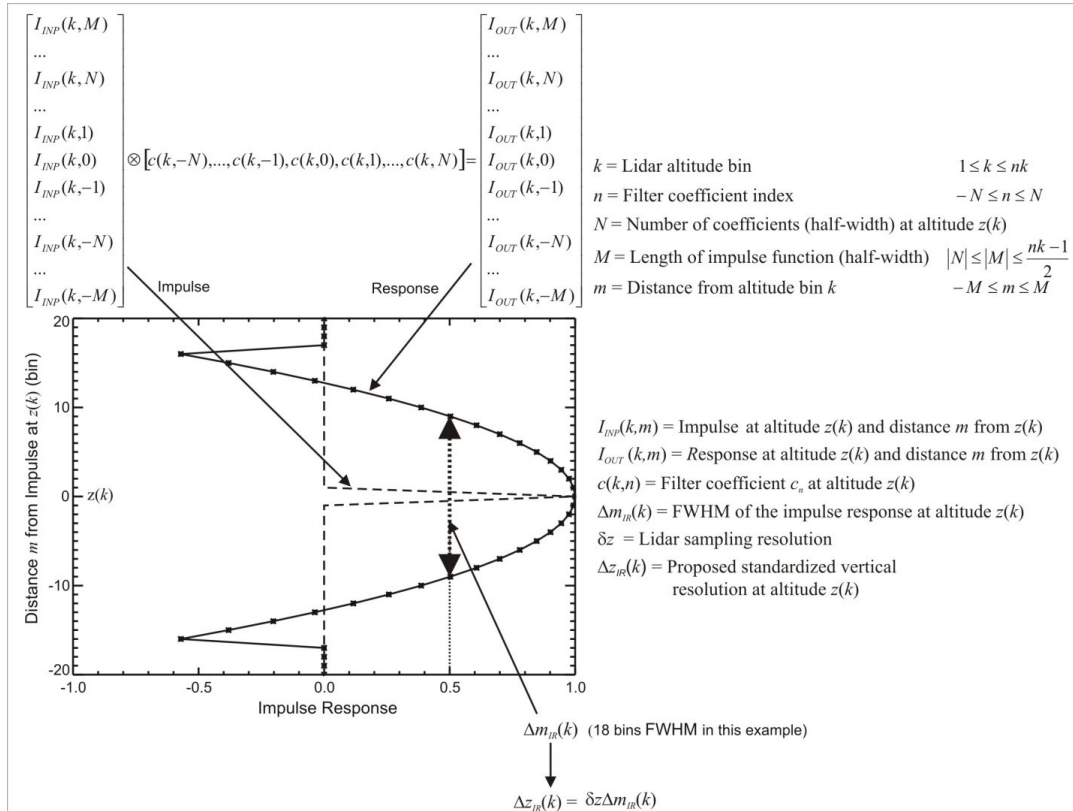


Figure 6: Schematics summarizing the procedure to follow to compute the standardized vertical resolution with a definition based on the impulse response FWHM Δz_{IR}

5

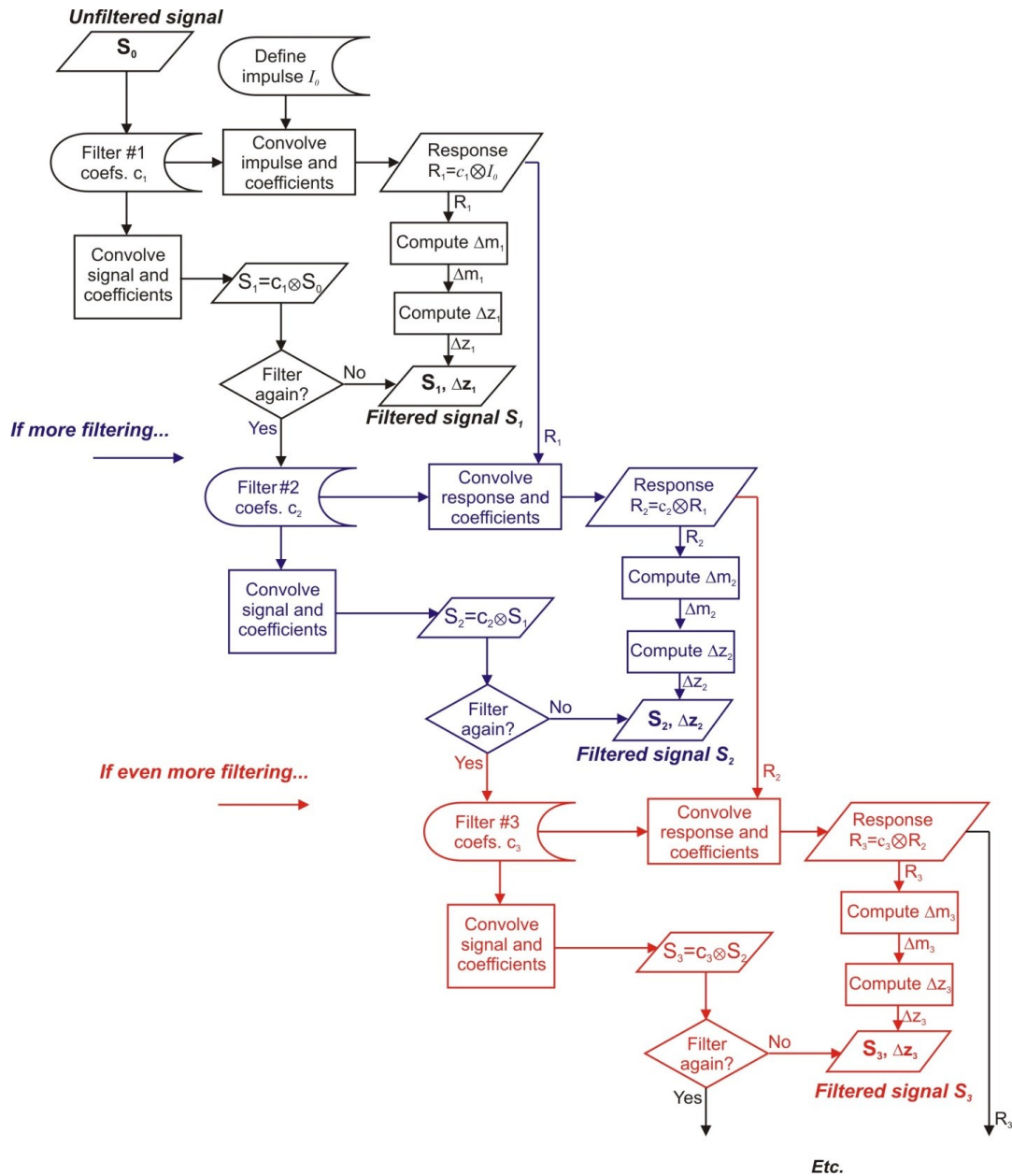


Figure 7: Schematics summarizing the procedure to follow to compute the standardized vertical resolution with a definition based on impulse response when the signal or profile is filtered multiple times

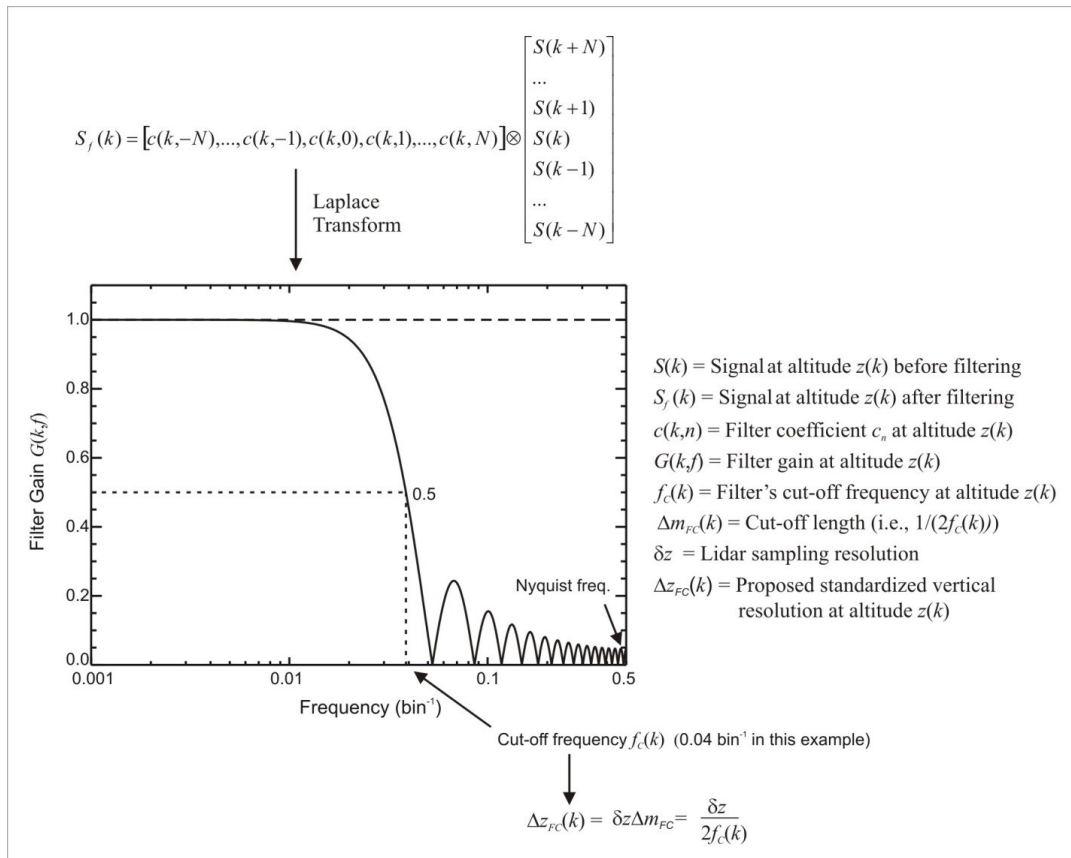


Figure 8: Schematics summarizing the procedure to follow to compute the standardized vertical resolution with a definition based on cut-off frequency Δz_{FC}

5

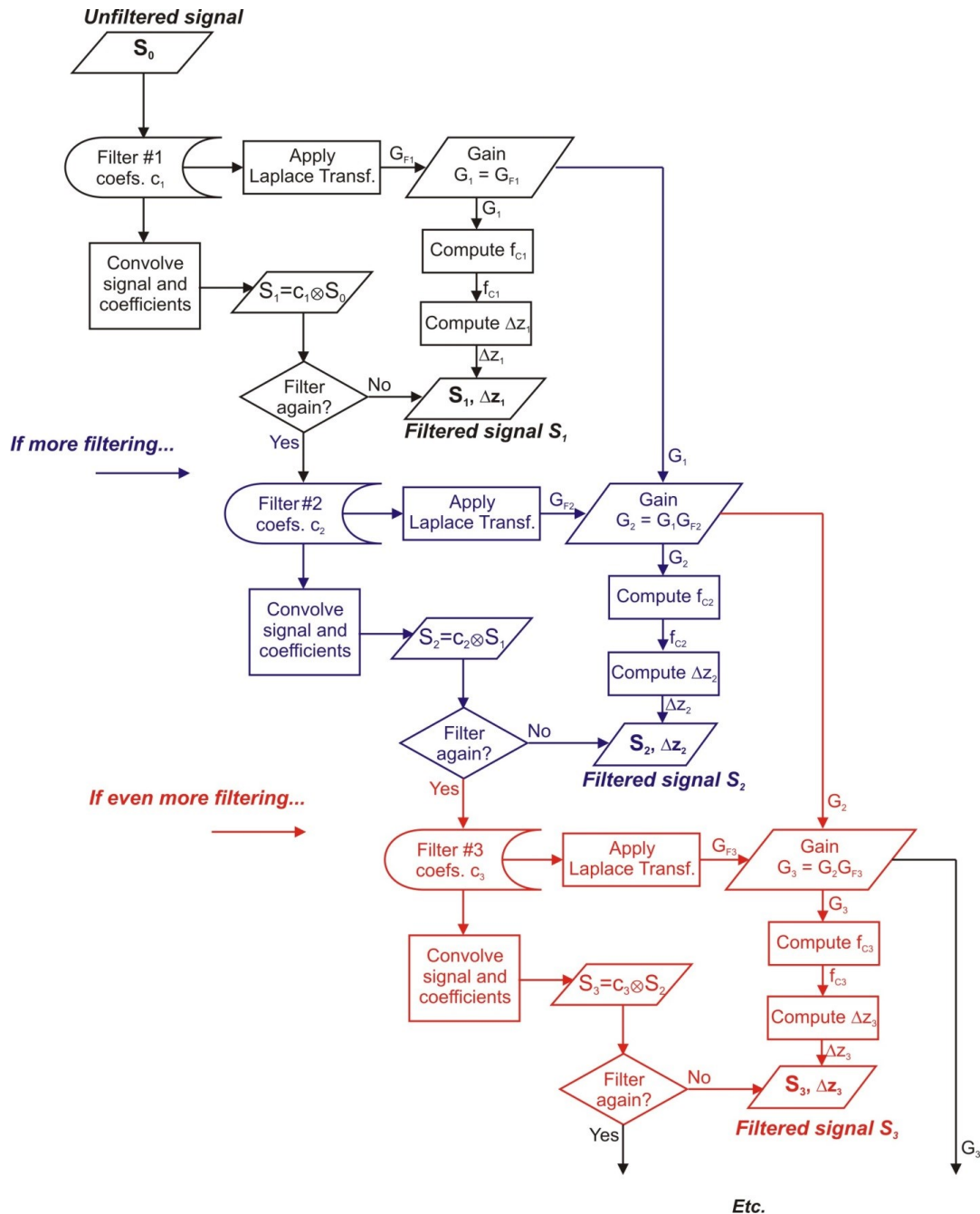
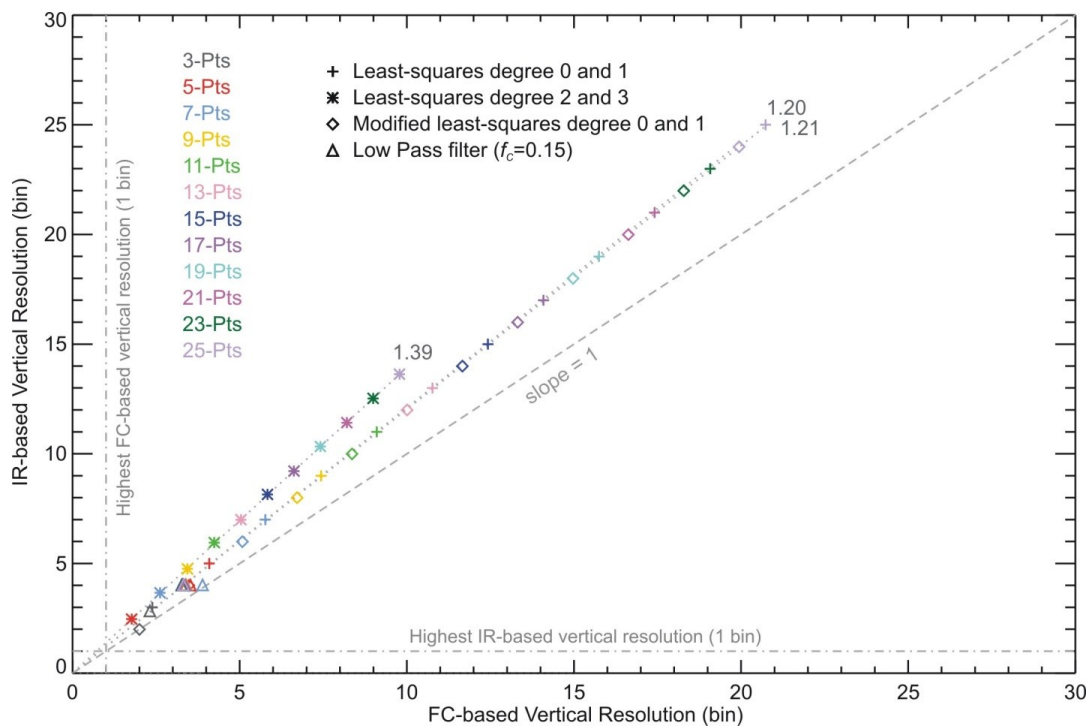


Figure 9: Schematics summarizing the procedure to follow to compute the standardized vertical resolution with a definition based on cut-off frequency when the signal or profile is filtered multiple times



5 **Figure 10 Comparison between the cut-off frequency-based and the impulse response-based standardized vertical resolutions for several smoothing filters introduced in section 2 and in the Supplement. The numbers at the end of the dotted straight lines indicate the proportionality constant (slope) between the 2 definitions for three of the four types of filters used. There is no such proportionality for the low-pass filter (prescribed cut-off frequency)**

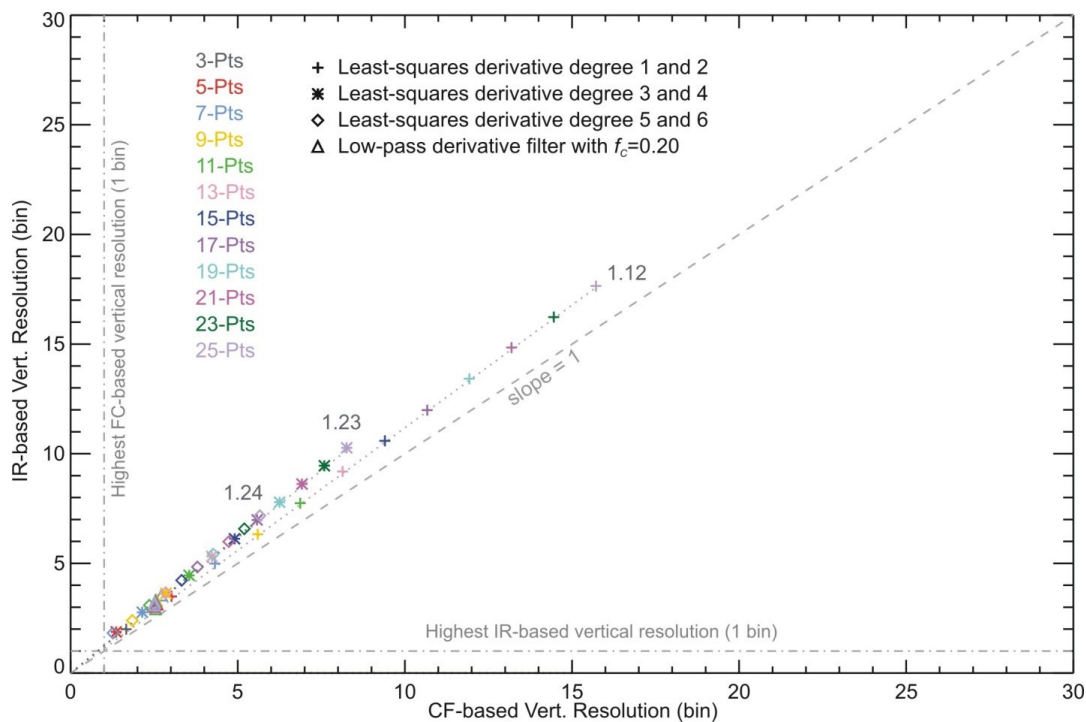


Figure 11: Same as Figure 10, but for derivative filters (section 2 and Supplement)

5

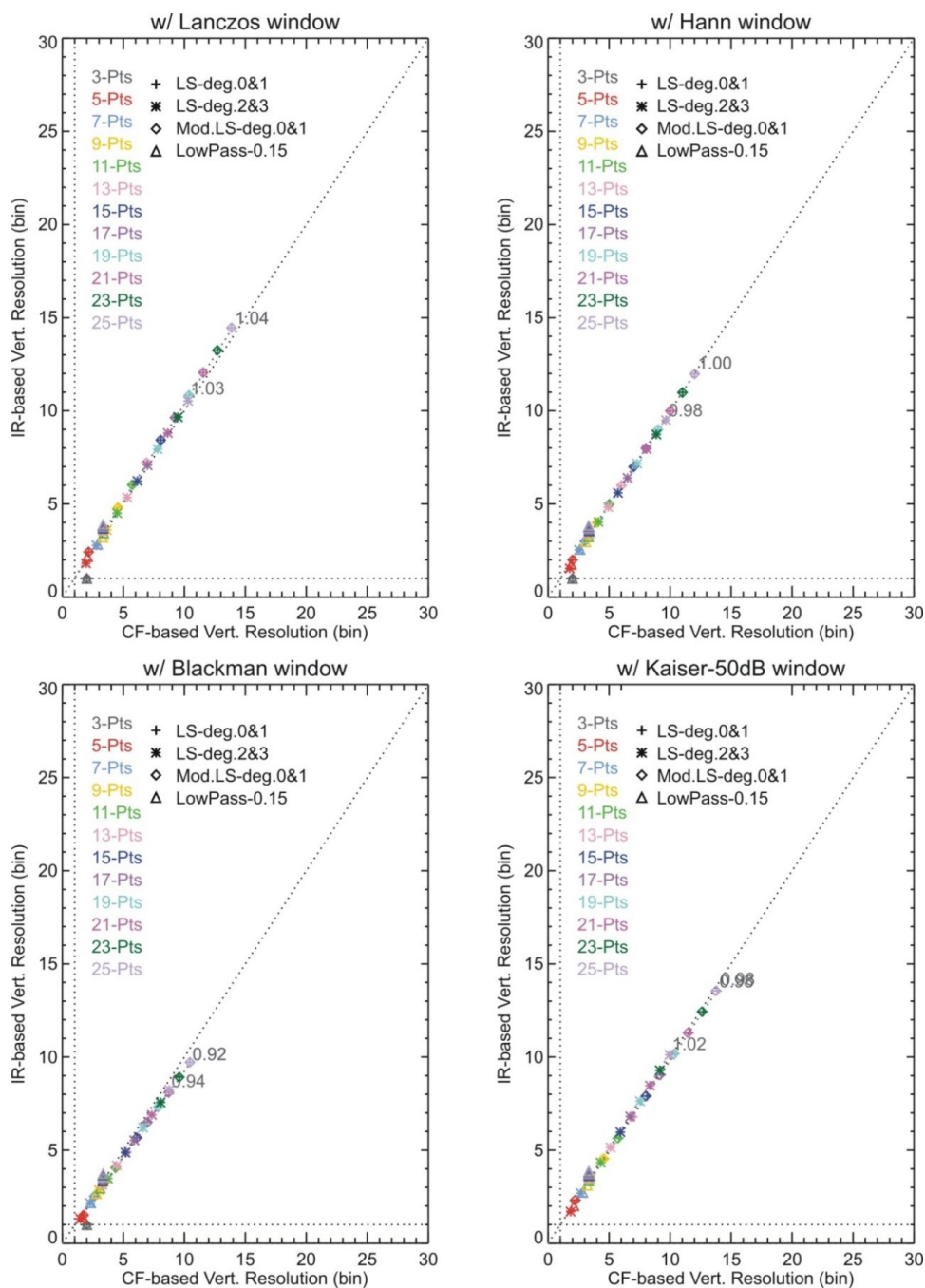
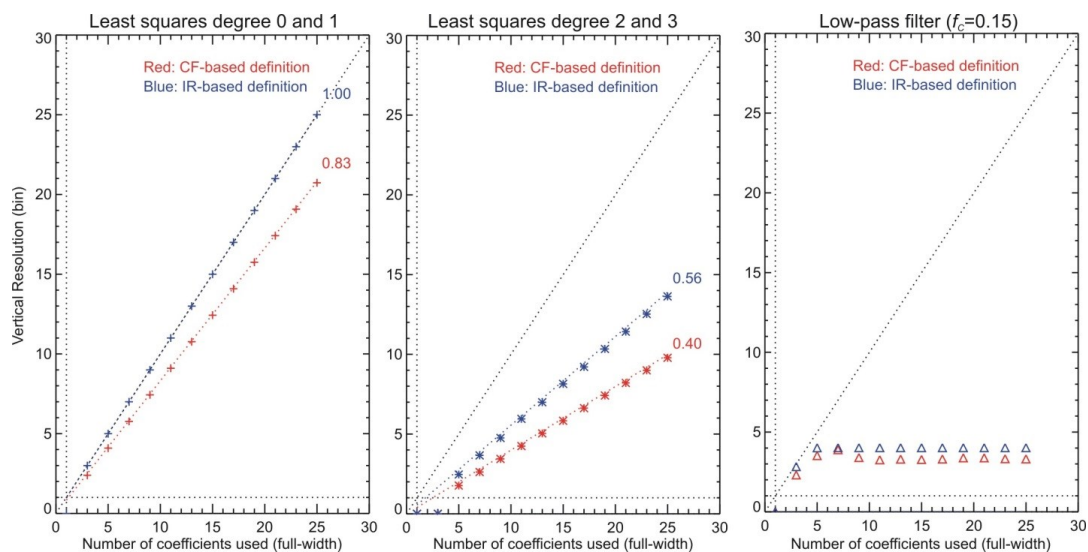


Figure 12: Same as Figure 10, but the filters being convolved with the four windows introduced in the Supplement



5 **Figure 13: Correspondence between cut-off frequency-based (red) and impulse response-based (blue) vertical resolution (in bins), and the number of filter coefficients used (full-width), for 3 filters introduced in section 2. The dashed grey line represents unity slope (i.e., 1 bin for 1 point), and the numbers at the end of the red and blue dotted straight lines indicate the slope of the linear fit applied to the paired points for each definition**

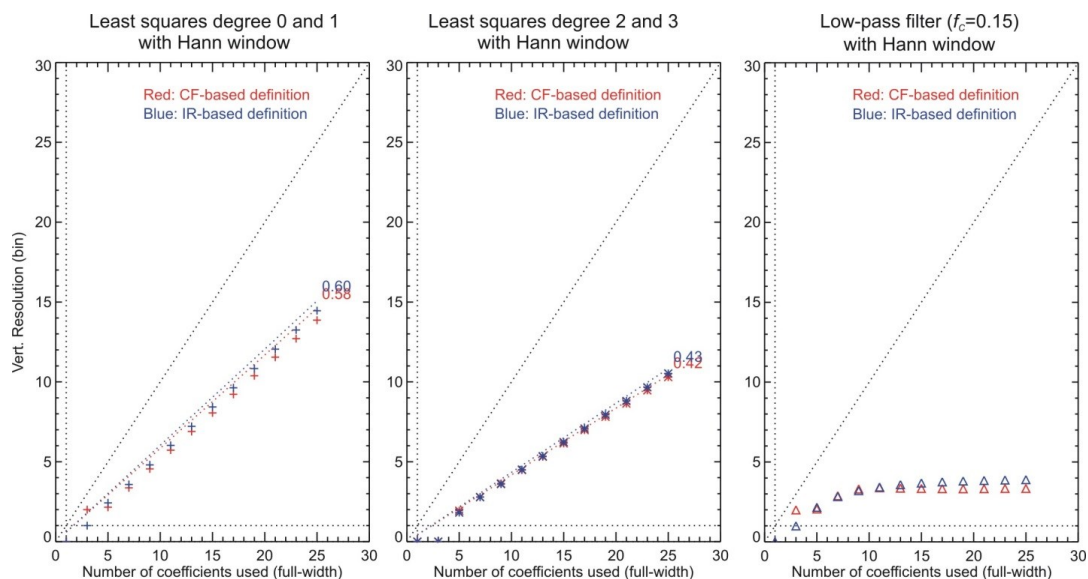


Figure 14: Same as Figure 13 this time after convolution by a von Hann window

5

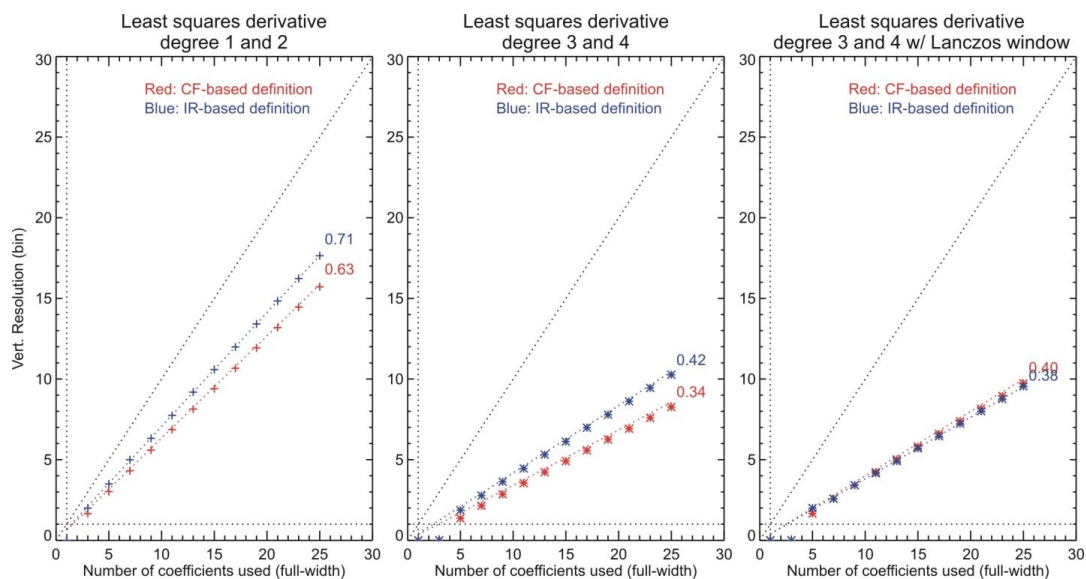


Figure 15: Same as Figure 13 but for selected derivative filters and windows from section 2 and Supplement